



ADDIS ABABA UNIVERSITY
School of Graduate Studies
Africa Centre of Excellence for Water Management
Master of Science Thesis

**THE IMPACT OF HYDROLOGICAL PARAMETERS AND CLIMATE INPUTS ON
EXTREME STREAMFLOW SIMULATION IN UPPER AWASH RIVER BASIN**

BY
METSIHET MEZGEBU WELDEMICHAEL

A Thesis submitted to Addis Ababa University School of Graduate Studies, Africa Centre of Excellence for Water Management, Hydrology and Water Resource Department in partial fulfillment of the requirement for the Degree of Master of Science.

In
HYDROLOGY AND WATER RESOURCES MANAGEMENT

Dr. Hadush Kidane Meresa (Advisor)

ACEWM/AAU, ETHIOPIA.
June 8, 2021



ADDIS ABABA UNIVERSITY
School of Graduate Studies
Africa Centre of Excellence for Water Management

The impact of hydrological parameters and climate inputs on extreme stream flow simulation in upper Awash River Basin

By
Metsihet Mezgebu

APPROVAL SHEET BY THESIS ADVISOR

This Thesis has been approved on the date shown below

.....
Dr. Hadush Kidane Meresa
(Advisor)

.....
Date

ACKNOWLEDGEMENTS

First and foremost, honor is to the Almighty God who blessed and taking care of me and my family and who enabled me accomplish this thesis work.

A special thanks to Dr. Hadush Kidane, this thesis work would not have been realized without the assistance and full support of him. Also I would like to thank Mr. Hailay Zeray for his contribution.

My appreciation goes as well to the Addis Ababa University ACEWM project community for the opportunity given to me and financial support to thesis research work. And I extended thanks to the Ministry of Water Resources, Awash River Basin Authority, and National Meteorological Agency for their cooperation in providing me with the necessary data for this research work.

Finally, I would like to owe many thanks to my family and all my friends for their endless support.

.

DECLARATION

I declare that this dissertation is my own original work and that it has not been presented and will not be presented by me to any other University for similar or any other degree award.

Signature: -----

COPYRIGHT

This dissertation is a copyright material protected under the Berne convention, the copyright Act 1999 and other international and national enactments, in that behalf, on intellectual property. It may not be reproduced by any means, in full or in part for research or private study, critical scholarly review or discourse with an acknowledgement, without written permission of the directorate of post graduate studies, on behalf of both the author and Addis Ababa University.

Dedication

To my Family, Elias Kebede, Nathan Elias and Estifanos Elias.

ABSTRACT

Quantifying possible sources of uncertainty in simulations of hydrological extreme events is very important for better risk management in extreme situations and water resource planning. The main objective of this research work is to identify and address the role of input data quality and hydrological parameter sets, and uncertainty propagation in hydrological extremes estimation. This includes identifying and estimating their contribution to flood and low flow magnitude using two objective functions Nash-Sutcliffe efficiency for flood and Log Nash-Sutcliffe efficiency for low flow, 20, 000 Hydrological ByransVattenBalansa Vdelning hydrological parameter sets, and three frequency distribution models (Log-Normal, Pearson-III, and Generalized Extreme Value). The influence of uncertainty on the simulated flow is not uniform across all the selected three catchments due to different flow regimes and runoff generation mechanisms. The result shows that the uncertainty in high flow frequency modeling mainly comes from the input data quality. In the modeling of low flow frequency, the main contributor to the total uncertainty is model parameterization. The total uncertainty of QT90 (extreme peak flow quintile at 90-year return period) quintile shows that the interaction of input data and hydrological parameter sets has a significant role in the total uncertainty. In contrast, in the QT10 (extreme low flow quintile at 10-year return period) estimation, the input data quality and hydrological parameters significantly impact the total uncertainty. This implies that the main factors and their interactions may cause considerable risk in water resources management and flood and drought risk management. Therefore, neglecting these factors and their interaction in disaster risk management, water resource planning, and evaluation of environmental impact assessment is not feasible and may lead to big risk.

Keywords: uncertainty, propagation, GLUE(Generalize likelihood uncertainty estimation, ANOVA(Analysis of variance), hydrological model extremes, HBV(Hydrological Byrans Vatten balansavdelning)

TABLE OF CONTENTS

ACKNOWLEDGEMENTS	iii
ABSTRACT.....	vii
LIST OF FIGURES	x
LIST OF TABLES.....	xi
LIST OF EQUATIONS	xii
ABREVIATION.....	xiii
1. INTRODUCTION	1
1.1 Background	1
1.2 Statement of problem.....	3
1.3 General and specific objectives.....	4
1.3.1. General objective	4
1.3.2. Specific objectives	5
1.4 Significance of the study.....	5
1.5. Scope and Limitation of the Study.....	6
2. LITERATURE REVIEW	7
2.1 Hydrological and Climate Variability.....	7
2.2 Interrelationship between climate and hydrology extremes	8
2.3 Implication of hydro-climate variability on flood and drought	9
2.4 Hydrological extreme Simulation Modeling.....	12
2.4.1 Conceptual Models	15
2.4.2 Physically based distributed models	16
2.5 Uncertainty in hydrological extremes	17
2.5.1 Model parameters Uncertainty.....	18
2.5.2 Estimating uncertainty propagation	19
2.6 Extreme flow Analysis.....	20
2.6.1 Flood Frequency Analysis techniques	20
2.7 Extreme frequency Probability distribution models	22

3.	STUDY AREA DESCRIPTION.....	25
3.1	Location	25
3.2	Land Use and Land Cover	26
3.3	Climate.....	26
3.4	study areas characteristics and input datasets	27
4.	METHODOLOGY	28
4.1	Modeling and numerical Techniques Design.....	28
4.2	Input data ensemble generation and modeling: Precipitation and temperature.....	29
4.3	Hydrological extreme modeling.....	30
4.3.1.	Conceptual modeling	30
4.3.2	Hydrological model parameter evaluation.....	32
4.4	Evaluation of ensemble simulations	33
4.5	Extreme Frequency Analysis (EFA).....	33
4.5.1	Generalize Likelihood Uncertainty Estimation (GLUE)	34
4.5.2	Uncertainty decomposition	35
5.	RESULTS	36
4.1	Ensemble of input precipitation and temperature evaluation.....	36
4.2	Calibration and Validation of Hydrological model.....	37
4.3	Evaluation of role and its associated uncertainty	39
4.4	Uncertainty decomposition using their variances	41
5	DISCUSSION	43
6	CONCLUSIONS.....	46
7	RECOMMENDATIONS	48
8	REFERENCES	50
9	ANNEX.....	57

LIST OF FIGURES

FIGURE 1. LOCATION AND MAP OF UPPER AWASH RIVER BASIN..... 25

FIGURE 2. STUDY LOCATIONS AND MAP OF STUDY AREAS (UPPER AWASH BASIN) **ERROR! BOOKMARK NOT DEFINED.**

FIGURE 3. DESIGNED COMPUTATIONAL FLOW CHART OF THE RESEARCH 29

FIGURE 4. THE CONFIDENCE BAND OF THE HIGHEST 1000 GENERATED PRECIPITATION TIME SERIES WITH A RESPECTIVE BOXPLOT OF THE COEFFICIENT OF DETERMINATION (RR). THE GREEN SHADED AREA IS A 95% CI OF DAILY PRECIPITATION (PRECI), AND ORANGE IS FOR DAILY AIR TEMPERATURE (TEMP). 36

FIGURE 5. BOUNDED NSE FOR PEAK FLOW (Y-AXIS) AND LOGNSE FOR LOW FLOW EVALUATION (X-AXIS) RESULTS FOR THREE CATCHMENTS FROM BEST/BEHAVIORAL SIMULATIONS OF HBV HYDROLOGICAL MODEL. 38

FIGURE 6. HYDROLOGICAL PARAMETER UNCERTAINTY AND ITS BAND ON SIMULATION OF EXTREME MONTHLY HIGH FLOW (LEFT COLUMN) AND MONTHLY MIN FLOW (RIGHT COLUMN) USING HBV MODEL. EACH COLOR STANDS FOR THE 95% CONFIDENCE INTERVAL OF 100 SIMULATIONS FROM 100 BEST HYDROLOGICAL PARAMETERS. THE RED DOT REPRESENTS THE OBSERVED EXTREME MAXIMUM/MINIMUM FLOW OF RESPECTIVE STATIONS, AND THE BLACK DOT STANDS FOR THE MEDIAN OF THE SIMULATED FLOW. 39

FIGURE 7. AGGREGATED UNCERTAINTY OF PEAK FLOW QUINTILE’S (LEFT COLUMN) AND LOW FLOW QUINTILE’S (RIGHT COLUMN) FOR THREE CATCHMENTS BASED ON 30 YEARS OF SIMULATED DATA. EACH SOURCE OF UNCERTAINTY IS PRESENTED BY EACH COLOR SHADE (THE COLORS ARE ADDITIVE): BLUE REPRESENTS DUE TO INPUT DATA AND FOR RANGE SHADED COLOR FOR HYDROLOGICAL PARAMETERS. THEIR CORRESPONDING MEDIAN VALUES ARE PRESENTED IN SOLID LINES OF RESPECTIVE UNCERTAINTY BANDS COLOR: BLUE LINE, AND ORANGE LINE, RESPECTIVELY, AND IN LOW FLOW FREQUENCY SIMULATIONS (LEFT COLUMN), THE GREEN SHADED AREA REPRESENTS INPUT DATA ROLE AND LIGHT ORANGE SHADED ARE FOR HYDROLOGICAL PARAMETERS. 40

FIGURE 8. THE SHARES OF UNCERTAINTY RELATED TO HYD PARS-HYDROLOGICAL PARAMETERS AND INPUT-INPUT DATA AND THEIR INTERACTION TERMS (INPUT*HYD PARS-HYDROLOGICAL PARAMETERS AND INPUT DATA) FOR THE SELECTED THREE CATCHMENTS AT QT90 (EXTREME PEAK FLOW QUANTILE AT 90 YEARS RETURN PERIOD – LEFT COLUMN) FOR THE SELECTED THREE CATCHMENTS AT QT10 (EXTREME LOW FLOW QUANTILE AT 10-YEAR RETURN PERIOD – RIGHT COLUMN). 42

FIGURE 9. SENSITIVITY OF HYDROLOGICAL MODEL RANKS USING RELATIVE MAXIMUM VERTICAL DIFFERENCE (MVD) VALUES OF THE HBV MODEL PARAMETERS IMPLEMENTED IN U/S KOKA, AKAKI, AND MELKA K RIVER STATIONS FOR HIGH FLOW (UPPER) AND LOW FLOW..... 43

LIST OF TABLES

TABLE 1. THE STATISTICAL DESCRIPTION OF OBSERVED STREAM FLOW AND PRECIPITATION IN 1981-2010.....	27
TABLE 2. RANGE OF HYDROLOGICAL PARAMETERS OF HBV MODEL AND L STANDS FOR LOWER VALUE AND U FOR THE UPPER PART OF THE MODEL PARAMETERS	31

LIST OF EQUATIONS

$PPE_{n,j} = PPO_n * EPE_{n,j}; \text{ where } EPE_{n,j} \approx N(0.01, \sigma_p^2)$	EQUATION 129
$TTE_{n,j} = TTO_n + ETE_{n,j}; \text{ where } ETE_{n,j} \approx N(\mu_t, \sigma_t^2)$	EQUATION 2.....29
$\frac{dS}{dt} = P + ET + Q_s - G_W$	EQUATION 3.....30
$NSE = 1 - \frac{\sum_{t=1}^j (Q_{o,t} - Q_{m,t})^2}{\sum_{t=1}^j (Q_{o,t} - \bar{Q}_o)^2}$	EQUATION 4.....32
$LogNSE = 1 - \frac{\sum_{t=1}^j (\log(Q_{o,t}) - \log(Q_{m,t}))^2}{\sum_{t=1}^j (\log(Q_{o,t}) - \overline{\log(Q_{o,t})})^2}$	EQUATION 533
$PCI = \left[1 - \left \left(\frac{NQ_{i,p}}{T} - 0.95 \right) \right \right] * \frac{1}{T} * \left[\left(\sum \frac{L_{u,t,p} - L_{l,t,p}}{Q_{o,T}} \right) \right]$	EQUATION 6.....33
LOG-NORMAL $f(x) = \frac{\exp(-\frac{1}{2}(\frac{\ln x - \mu}{\sigma})^2)}{x\sigma\sqrt{2\pi}}$	$\Sigma, \mu (\Sigma > 0)$ EQUATION 734
PEARSON-III $f(x) = \frac{(x-\gamma)^{\alpha-1}}{\beta^\alpha \Gamma(\alpha)} \exp\left(-\frac{x-\gamma}{\beta}\right)$	$A, B, \gamma (A > 0, B > 0)$ EQUATION 8.....34
GEV $f(x) = \begin{cases} \frac{1}{\sigma} \exp(-(1+kz)^{-\frac{1}{k}}) (1+kz)^{-1-\frac{1}{k}} & k \neq 0 \\ \frac{1}{\sigma} \exp(-z - \exp(-z)) & k = 0 \end{cases}$	$K, \Sigma, \mu (\Sigma > 0)$
EQUATION 9.....	34
$Z(X) = 1 - \frac{\sigma_0^2}{\sigma_e^2}$	EQUATION 1035
$SST = SS_{ID} + SS_{HP} + SS_{IDHP} + Error$	EQUATION 11.....35

ABBREVIATION

ANOVA	ANALYSIS OF VARIANCE
DEM	DIGITAL ELEVATION MODEL
DSS	DECISION SUPPORT SYSTEM
EPA	ENVIRONMENTAL PROTECTION AGENCY
ESCAP	UNITED NATIONS ECONOMIC AND SOCIAL COMMISSION FOR ASIA AND PACIFIC
FAO	FOOD AND AGRICULTURE ORGANIZATION
FAOSTAT	STATISTICS FOOD AND AGRICULTURE ORGANIZATION
FFEW	FLOOD FORECASTING AND EARLY WARNING
FFWS	FLOOD FORECASTING AND WARNING SYSTEM
CMPI5	Coupled Model Inter comparison Project Phase 5
GIS	GEOGRAPHIC INFORMATION SYSTEM
GPS	GLOBAL POSITIONING SYSTEM
GLUE	GENERALIZE LIKELIHOOD UNCERTAINTY ESTIMATION
HBV	HYDROLOGICAL BYRANS VATTENBALANSAVDELNING
HEC-HMS	HYDROLOGICAL ENGINEERING CENTRE – HYDROLOGIC MODELLING SYSTEM
IPCC	INTERGOVERNMENTAL PANEL FOR CLIMATE CHANGE
ITCZ	INTER TROPICAL CONVERGENT ZONE
MAPE	MEAN ABSOLUTE PERCENTAGE OF ERROR
MSE	MEAN SUM OF ERROR
RMSE	ROOT MEAN SQUARE ERROR
MCS-GLUE	MONTE CARLO SIMULATION GENERALIZE LIKELIHOOD UNCERTAINTY ESTIMATION
SSE	SUM SQUARE OF ERROR
NSE	NASH-SUTCLIFFE EFFICIENCY
GEV	GENERALIZED EXTREME VALUE.
PDF	PROBABILITY DENSITY FUNCTION
PCI	CONFIDENCE INTERVAL PRINCIPLE
UNEP	UNITED NATION ENVIRONMENTAL PROTECTION
UNISDR	UNITED NATIONS INTERNATIONAL STRATEGY FOR DISASTER REDUCTION
WMO	WORLD METEOROLOGICAL ORGANIZATION

1. INTRODUCTION

1.1 *Background*

The accuracy and reliability of river flow predictions are essential for extreme water management, policy-making, and water allocation as well as integrated and sustainable water resource management practices (disaster management, irrigation management, hydropower regulation, environmental flow) (Meresa and Romanowicz, 2017; Meresa, 2019; Okoli et al., 2019). The precision and trustworthiness of river flow model predictions and extreme frequencies are affected by different factors such as results from hydrological model input variables (such as temperature and precipitation Bae et al., 2018), conceptual model structures (Mockler et al., 2016; Vetter et al., 2017), model parameters, and extreme frequency distributions (Meresa and Romanowicz, 2017). Defining and estimating the critical uncertainty sources at each stage from input data to frequency of hydrological extremes is important to have a comprehensive understanding of the role of systematic and inherent errors. The nonlinear and inerascable uncertainty propagation character requires quantifying the uncertainty level at each stage, starting from the model inputs (precipitation and temperature) to the low flow and flood frequencies for better water extreme management and infrastructure construction (e.g. Reservoirs, flood protection walls, flood zoning).

Defining and estimating uncertainty propagation in extreme hydrological modeling processes is critical for water resource planning, extreme risk management. The hydrological community has identified the propagation of uncertainty as one of the 23 unsolved problems in hydrology (Blöschl et al., 2019). Numerous actors in water resource and hydrologic research have attempted to identify different sources of uncertainty in water resources (Xu et al., 2010; Vetter et al., 2017; Kusangaya et al., 2018; Prein, 2019) and extreme hydrological frequencies (Vrugt et al., 2008; Zhang et al., 2016; Qi et al., 2016; Sun et al., 2017; Hattermann et al., 2018; Her et al., 2019). Therefore, this research work has addressed uncertainty in water resources and extreme hydrological modeling in the isolated form, whereas an integrated framework is required to evaluate the critical sources in projected high and low flow. For example, Kavetski et al. (2006) examined input uncertainty in hydrological modeling using a Bayesian approach in two catchments in North America. Similarly, Her et al. (2019) branded three sources of uncertainty using Analysis Of Variance Analysis (ANOVA), hydrological structure, parameters, and climate models. Hence, researchers found

that climate models have significant contribution to extreme hydrological conditions. They strongly recommended incorporating input uncertainty in Ohio River basin. Chen et al. (2013) evaluated the role of hydrological model structure and parameter uncertainties in extreme hydrological regime simulations. They found that the sources have significant contribution to the high flow in selected catchments in China. Prein, (2019) stated that the extreme precipitation events and their implication on intense hydrologic cycle could highly expose to uncertainty.

Similarly, Sun et al. (2017) identified multiple sources of uncertainty (distribution types, distribution parameters, and peak over threshold) in flood frequency. They found that distribution types could play a significant role in controlling the flood magnitude. Zhang et al. (2016) also did an uncertainty investigation in snow-dominated catchments from China. They found that input data's role is more significant than the role of the hydrological parameter in peak flow estimation. Others have investigated the uncertainty caused by input and hydrological parameters (e.g Zhang et al., 2016; Bae et al., 2018), hydrological parameters and model structure (e.g., Butts et al., 2004; Jin et al., 2010), climate change, and hydrological parameters (e.g., Krysanova et al., 2018; Her et al., 2019; Meresa, 2019), climate change and flood frequency (e.g., Qi et al., 2016a; Meresa and Romanowicz, 2017), frequency distribution parameters and types (e.g., Sun et al., 2017). These studies have shown that only one aspect of systematic and/or inherent uncertainty is not enough to address the problem in estimating extreme flow. However, the uncertainty propagation at different stages and levels is not widely studied(Matron and Paseka, 2017; Kiang et al., 2018). This uncertainty propagation comprises input data, hydrological parameters, and extreme probability distribution types.

The accuracy of meteorological variables can be impacted by systematic, instrumental errors and external factors(Karakoram, 2016;Yen et al., 2018); parameter representation and instability of hydrological models may lead to significant error in timing and magnitude of hydrological process and regimes (Zhang et al., 2016; Bae et al., 2018); simplification of the real watershed processes is another source of error in water resource modeling (Song et al., 2015; Meresa and Gatachew, 2018) and difficult to represent in a single model, which is mainly due to the lack of precise mathematical principles, catchment heterogeneity and complexity of water cycle (Jiang et al., 2017; Emam et al., 2018). The frequency-magnitude relationship is also strongly influenced by distribution type and parameters (Ham et al., 2017), and only one extreme distribution may lead to a certain level of uncertainty. All these

important factors can have an error in high and low flow design value simulation and associated with higher risk level in extreme management and planning.

Hence, the extreme events likelihood occurrences and their uncertainty probability as well distributions using HBV model parameter simulation were not well addressed in the area. Thus, by predicting the uncertainty effects of hydrological extremes for Upper Awash River Basin using strong prediction and simulation technique was enabled to investigate about the hydrological extreme responses into water resource planning and development decision tools to some future scenario.

Thus this research work mainly concerned to identifying the role of the input data and hydrological parameter sets; address their critical uncertainty sources in extreme flow simulations (flood and low flow). Also a comprehensive uncertainty framework using generated plausible rainfall characteristics developed and combines them with hydrological parameters to assess extreme frequency using different distribution models. Therefore, this novel approach combines statistical climate ensembles, multiple parameter sets of HBV hydrological model and three flood frequency distribution models to investigate the interplay among the associated uncertainty in high and low flow modeling.

1.2 Statement of problem

Hydrological models was designed to answer a specific water-related question and to predict a high-flow or low-flow periods (IPCC a, 2014; Koster et al., 2017; Lakshmi et al., 2001; Mosavi et al., 2018; Pechlivanidis et al., 2017; WMO, 2018, 2019). Hence, to assess the change on hydrological extremes, hydrological models have a big role and very important tools to simulate and predict events in hydrological cycle. The ability of such models to simulate the high and low flow events are important for planning and management of risk-based water resources planning applications (ESCAP, 2017; Jain et al., 2018; World Meteorological Organization, 2011b). However, Hydrological model needs to be evaluated its output results and quantify their efficiency for flow prediction.

Moreover, the uncertainties estimating are likely to be magnified during extreme events and such limitations must be taken into account (WMO, 2018, 2019). Thus, accurate assessment of the parameters and predictive uncertainty of hydrological model was an important aspect of any hydrologic modeling application (Schoups G. , Vrugt, Fenicia, & Giesen, 2010). According to (Koutsoyiannis & Montanari, 2007), an appropriate modeling approach for any

uncertain hydrological system should necessarily include quantification of its uncertainty within a stochastic framework. Hydrological modeling uncertainty is traditionally recognized within the model calibration and validation phases as stated by (Beven & Binley, 1992). Similarly, (Keating, John, A., & Qinjun, 2010) concluded that Uncertainty quantification bring attentions of researchers try to understand which parts of our models are well resolved, and which parts of our process knowledge and theories are subject to considerable uncertainty, and as decision-makers push to better quantify accuracy and precision of model predictions (Beven & Beven, 2007; Beven & Binley, 1992, 2014).

Mostly in Ethiopia high flow occurred from torrential rainfall and the topography of the highland mountains and lowland plains with natural drainage systems which formed by the principal river basins (Awulachew et al., 2011; Bae et al., 2018; Breinl et al., 2017; Desta & Lemma, 2017; Dietrich et al., 2008; Emam et al., 2018; Gebrehiwot et al., 2011; Hadush K Meresa & Gatachew, 2016; Taye & Willems, 2012). Therefore, hydrological extremes with high flood and low flow uncertainty is an important problem occurred in Upper Awash River Basin (Bewket et al., 2015; Shawul et al., 2019; Tadese et al., 2019). Hence, the extreme events likelihood occurrences and their uncertainty probability as well distributions using HBV model parameter simulation were not well addressed in the area.

Therefore, this research was identifying the intensities of uncertainty prediction techniques for better decision tools that target to determine the high and low flood frequencies distribution and impact of HBV model parameters performance in response to accurate river flow simulation of Upper Awash River Basin mainly Akaki, MelkaKunture and Upstream Koka sub basins as well .

1.3 General and specific objectives

1.3.1. General objective

The General objective of this research is to identify the role of the input data and hydrological parameter sets and address their critical uncertainty sources in extreme flow simulations (flood and low flow) using combined statistical climate ensembles, multiple parameter sets of HBV hydrological model and three flood frequency distribution models to investigate the interplay among the associated uncertainty in high and low flow modeling in Upper Awash Basin.

1.3.2. Specific objectives

- To identify the role of the input data and hydrological parameter sets and address their critical uncertainty sources in extreme flow simulations (flood and low flow) in Upper Awash River Basin.
- To assess extreme frequency using generated plausible rainfall characteristics and three different distribution models combines them with hydrological parameters.
- To investigate the combined statistical climate ensembles, multiple parameter sets of HBV hydrological model and three flood frequency distribution models associated to uncertainty in high and low flow modeling.

1.4 *Significance of the study*

Upper Awash River Basin is one of the repeatedly flooding prone areas in the Ethiopia. Hence, studying hydrological extreme phenomena was very important to reduce risks with economic loss and water resource planning associated infrastructure development. To solve this problem hydrological model best fit with accurate and efficient techniques must be established to monitor flow regime fluctuation and predict uncertainty in the selected catchments such as, Akaki, Melka kunture and Upstream Koka. According to (Murphy, et al., 2004), un certainty analysis forms the basis for model comparison and selection allows identification water management strategies that take account of prediction uncertainties. Apart from predicting and guessing the quantity of water for decision makers, some models could also help in predicting the impacts of natural and anthropogenic changes as well as quantifying the spatial and temporal availability of the water resources (Alamgir et al., 2018; Austin et al., 2010; Matewos, 2019; Petersen, 2019; Taye et al., 2015; Vrugt et al., 2008).

Hence, HBV hydrologic model uncertainty prediction was evaluated with three frequency analysis techniques to simulate hydrological extremes of high flood and low flow distribution probability of Upper Awash watershed stream flow and the model procedure consist of computing event of high flood and low flow. Moreover, simulation and prediction using HBV hydrological model have been widely applied to measuring high flood and low flow response of model parameters for a watershed that uncertainties treated with capabilities of its performances (Koster et al., 2017; WMO, 2019). Therefore, this study has been conducted

to solve problem related to extreme flow at Akaki, Melka Kunture and upstream Koka. In the study area previously, few researches have been conducted on river flow simulation using different hydrological models (Dietrich et al., 2008; McCuen, 2016; Tadese et al., 2019; WMO, 2019). However, in this research HBV model with three distribution statistical methods was computed to identify best fit model parameters uncertainty to assess accurate and efficient hydrological extremes for strong decision tool technique for high flood and low flow prediction and simulation using temperature and precipitation as input data.

Therefore, this study has contributed best decision tool to stream flow prediction using HBV model which in turn contributes to the National flooding hazard mitigation strategies and water resource planning includes flood damage reduction, floodplain regulation, and systems operation (X. Chen et al., 2014; Hamdan et al., 2019; Jain et al., 2018; Rind, 1991; Vetter et al., 2017) in upper Awash Basin and study areas sub basins as well.

1.5.Scope and Limitation of the Study

This research work mainly concerned to identifying the role of the input data and hydrological parameter sets; to address their critical uncertainty sources in extreme flow simulations (flood and low flow) using HBV model. The uncertainty prediction was evaluated with three frequency analysis techniques (Log-normal, Pearson III and Generalized extreme value distribution). However, this study limited that, the hydrological and meteorological data quality (homogeneity analysis, consistency check) assessment. The HBV model was limited in low flow analysis.

2. LITERATURE REVIEW

2.1 Hydrological and Climate Variability

Climate change refers to any change in climate over time, whether due to natural variability or anthropogenic forces (Malone et al., 2010; Rind, 1991; World Meteorological Organization, 2011a, 2011b), and climate change or variability is highly complex and non-linear in how it reacts (IPCC a, 2014). Recent findings point to changes in the water cycle and in climatic variability (Adeloye & Montaseri, 2002; Devia et al., 2015; Pechlivanidis et al., 2017; WMO, 2018). While the climate tends to change quite slowly, that doesn't mean we don't experience shorter-term fluctuations on seasonal or multi-seasonal time scales (Khazaei & Ahmadi, 2013; Koster et al., 2017; Kusangaya et al., 2018; WMO, 2018; World Meteorological Organization, 2020). Climate change is exacerbating the natural hydrological variability, and hence presenting another dimension to the challenge of water resources development and management (ESCAP, 2017; Keshta et al., 2019; Silvis et al., 2019; Taylor, 2009; van den Hurk et al., 2016).

On the other hand, climate variability refers to variations in the mean state and other climate statistics (standard deviations, the occurrence of extremes, etc.) with temporal and spatial scales of weather events (H.K. Meresa & Romanowicz, 2017; Eva M. Mockler et al., 2016; Okali et al., 2019; Qi, Zhang, Fu, & Zhou, 2016). According to (IPCC a, 2014; McGregor, 2017; Rind, 1991), climate variability, and when scientists talk usually referring to time periods ranging from months to as many as 30 years. Hence, variability may result from natural internal processes within the climate system (internal variability) or from variations in natural or anthropogenic external forces (Low & Boettcher, 2020; Lynch & Cassano, 2006; McGregor, 2017; L. A. Melsen, 2017; Ramdane, 2014; World Meteorological Organization, 2011b).

Understanding the global hydrological cycle and how we use water is essential for planning a sustainable source of water for the future (Austin et al., 2010; Jannis et al., 2021; Malone et al., 2010; McGregor, 2017). Changes in the hydrological cycle have a direct impact on droughts, floods, water resources, and ecosystem services (ESCAP, 2017; Frederick & Major, 1997; Gitonga et al., 2020; IPCC a, 2014; McGregor, 2017; Petersen, 2019). Hydrological information requirements for flood forecasting and warning systems need to understand the

overall flood characteristics of the area as well as possessing real-time information for operations (Clark et al., 2017; Devia et al., 2015; L. Melsen et al., 2016; H.K. Meresa, 2019; Song et al., 2015; Tessema, 2011; Weeink, 2010). In recent years, advanced flood forecasting using a grid based hydrological catchment model with grid cells between 2 and 14km even higher resolution has been used for hydrological model based on coupling meteorological observations(Clark et al., 2017; Devia et al., 2015; Gao et al., 2016; Jenkins et al., 2019; Khazaei & Ahmadi, 2013; Krivoruchko & Team, 2012; Song et al., 2015).

Projecting the climate system in the spatial scales is difficult, both in the atmosphere and in the terrestrial surface (Clark et al., 2017; Devia et al., 2015; Gao et al., 2016; Jenkins et al., 2019; Khazaei & Ahmadi, 2013; Krivoruchko & Team, 2012; Machiwal & Jha, 2012; L. Melsen et al., 2016; Song et al., 2015). However, Trends in stream flow and projected water cycle changes analyzed in the Coupled Model Inter comparison Project Phase 5 (CMIP5; a climate evolution experiment involving multiple climate drivers performed by dozens of climate modeling groups) to forecast drought and flood risk (EPA, 2017; ESCAP, 2017; Koster et al., 2017).

Extreme hydrology system could be developed using a variety of techniques such as upstream and downstream river level correlation, rainfall to river level correlation, rainfall-runoff modeling, hydrodynamic modeling (X. Chen et al., 2014; Gautam & Consulting, 2014; Givati et al., 2019; Jain et al., 2018; Petersen, 2019; WMO, 2006; Wu et al., 2011) .

2.2 Interrelationship between climate and hydrology extremes

Extreme hydrological characteristics and available water resources, both in terms of quantity and quality (Bae et al., 2018; Elliot & Bonotto, 2017; Emam et al., 2018; Kourtis et al., 2019; Kusangaya et al., 2018;Masia et al., 2018; Meresa & Gatachew, 2016; Vesely et al., 2019; Yen et al., 2018), are significantly influenced by environmental changes, such as climate, land use, river engineering, construction of reservoirs, and mining activities. Hence, magnitude and frequency of hydrological extreme events such as drought and flooding, the significance of adequately modeling hydrological extreme events is fully recognized (Melesse et al., 2011; Meresa, 2019; Taye et al., 2015; Xu et al., 2010b).Moreover, estimation of extreme rainfall/flood for various return periods is of prime importance for hydrological design or risk assessment and changes in the hydrological cycle have a direct

impact on droughts, floods, water resources, and ecosystem services(X. Chen et al., 2014; EPA, 2017; Esau et al., 2021; Jain et al., 2018; Taylor, 2009).

Precipitation, evapotranspiration, and soil moisture patterns defined as climate change impacts have extreme effects on the hydrologic cycle (Emami & Koch, 2019; Givati et al., 2019; Jannis et al., 2021; McGregor, 2017; Szalińska et al., 2021). Like many countries ,climate change is one of the most important issues of Ethiopian climate since its rain-fed agriculture is largely dependent on the amount and regular onset of seasonal precipitation (Fazzini et al., 2015; Hadgu, 2015; Jury & Funk, 2013; Lemann et al., 2019; Melesse et al., 2011; Meresa, 2019; Hadush K Meresa & Gatachew, 2018; W. Taye et al., 2015). Knowledge about catchment's hydrological response is essential to predict the influences of climate change on future spatial and temporal water availability (Almeida et al., 2006; Fazzini et al., 2015; Hadush K Meresa & Gatachew, 2018; Onyutha, 2016; Sertel et al., 2019; Singh & Roy, 2002; Yihdego & Webb, 2013). Rainfall patterns might change with increasing temperature and drought occurs in some areas(Jain et al., 2018; Kidd & Huffman, 2011; McGregor, 2017; Rind, 1991).

However, total rainfall sometimes increases and heavy rainfall induces floods in Ethiopia mainly controlled by the seasonal migration of the ITCZ and by the complex topography of the country (Fazzini et al., 2015; Jury & Funk, 2013; Tadese et al., 2019; Tessema, 2011). This combination results in a variety of climate types and climate conditions that may vary also within a short distance (Fazzini et al., 2015). Moreover, climate of Ethiopia is mainly controlled by the seasonal migration of the ITCZ and by the complex topography of the country (Fazzini et al., 2015; Jury & Funk, 2013). Many mid-latitude arid and semi-arid regions are likely to receive less precipitation, with the likelihood of having droughts larger and longer than those observed since 1900 (Fazzini et al., 2015; Tadese et al., 2019).

2.3 Implication of hydro-climate variability on flood and drought

According to (IPCC a, 2014; Malone et al., 2010; McGregor, 2017; World Meteorological Organization, 2011b, 2013) , the continued increase in the greenhouse gas emissions will lead to the warming and changes in the various components of the climate system. With respect

to the hydrological system, these changes are reflected in the increased frequency and severity of risk-based water disasters such as drought and floods (WMO, 2018, 2019; World Meteorological Organization, 2020). Thus, Climate change has had various effects, including an increase in the frequency of extreme rainfall events (ESCAP, 2017; Gautam & Dulal, 2013; Rind, 1991; van den Hurk et al., 2016).

Changes in hydrological cycles are expected to be more severe in the 21st century due to increasing temperatures and the saturation vapor pressure (ESCAP, 2017; IPCC a, 2014; WMO, 2019). Climate variability and change affects many socio-economic sectors such as agriculture, water resources, forestry, fisheries, ecological systems, human settlements, and health, with significant effects on national food security (IPCC a, 2014; WMO, 2019). Water-related disasters are the most economically and socially destructive of all natural disasters (ESCAP, 2017; IPCC a, 2014; Ngarava et al., 2019; WMO, 2019). Global reported showed that floods, droughts and storms have affected 4.2 billion people and lost nearly USD 1.3 trillion of damage (WMO, 2018).

Similarly, climate change will also affect the function and operation of existing water infrastructure including hydropower, water supply, flood protection, irrigation and drainage as well as overall water management practices (Cruz et al., 2021; ESCAP, 2017; Hellin & Fisher, 2019; Jannis et al., 2021; Stonehouse, 2013; WMO, 2019; World Meteorological Organization, 2011b). Extreme weather events will occur more often, including drought, floods, coastal storms, and heat waves, increasing mortality and property damage (Austin et al., 2010; McGregor, 2017; Parker & Abatzoglou, 2019; Szalińska et al., 2021; Taylor, 2009; Petersen, 2019).

Climate change induced variations have significant social, economic, and environmental impacts in the form of crop failure, and degradation (Antle, 2008; Yalew et al., 2018). Moreover, Agriculture sector is strongly influenced by weather and climate, which in turn have impacts on agricultural production (Emerta & Aragie, 2013; Mancosu et al., 2015). Temperature and precipitation, as two important climatic variables for the evaluation of future grain yield (IPCC a, 2014). It is realized that projected climate change affect agriculture and induce significant yield reduction in the future due to climate variability (Thomas & Chiang, 2013). In addition certain effects of agricultural and industrial development, notably pollution and sedimentation, reduce water availability and amplify

vulnerability to extreme hydrological events (Austin et al., 2010; McGregor, 2017; Parker & Abatzoglou, 2019; Szalińska et al., 2021; Taylor, 2009; Petersen, 2019).

Similarly, changes in the hydrological cycle have a direct impact on droughts, floods, water resources, and ecosystem services (Ramdane, 2014; Tall et al., 2018). Temporal variability of rainfall is typically 40% around the mean -much higher than in temperate zones and the spatial distribution of rainfall is varied (IPCC a, 2014). More intense precipitation in wet tropical regions is likely to increase flood risk and large floods will probably surpass historical events in size and frequency in some regions (IPCC a, 2014).

Water scarcity, exacerbated by climate change could cost some regions up to 6% to their GDP (World Bank, 2016). Ethiopia is seriously threatened by climate change, which contributes to frequent drought, flooding, and rising average temperatures (Emerta & Aragie, 2013). The country will be vulnerable to Land productivity and crop yield is expected to decline as a result of climate change continuously throughout the period between 2030 and 2050 (GebreEgziabiher, Stage, Mekonnen, & Alemu, 2012). According to (Yalew et al., 2018) a close relationship between annual rainfall variability and agricultural GDP as well as affecting overall GDP growth. Hence, increased in temperatures, changes in rainfall amounts and patterns, also increased incidence of drought and flood events (Bewket et al., 2015).

Droughts in particular have had great impact on farmers' livelihoods (Emerta & Aragie, 2013; Yalew et al., 2018). In terms of impact on livelihoods, the 1984 and 2003 droughts affected 7.5 and 12.6 million people respectively (Murphy, n.d.). Moreover, the El Niño event in 2015/16 resulted in Ethiopia experiencing one of the worst droughts in decades, with over 10.2 million people estimated to be in need of food aid (Numbers, 2017; Study, n.d.). Thus, climate change could, therefore, lead to the near collapse of food production structures in Ethiopia and it is a significant threat to livelihoods since agriculture crops, livestock and fisheries (Hellin & Fisher, 2019).

On the other hand, climate change affects water resources in many rivers of the country (Tadese et al., 2019). Thus, due to high variability exhibited by the climate components over time and space are the main reason behind the spatial and temporal variability in the availability of water (Bewket et al., 2015; ESCAP, 2017; Winters et al., 1996; Yalew et al., 2018). Therefore, reduction of water yield against the slightly increasing rainfall projected for

much of the country indicates the effects of increased evapotranspiration loss of water due to the rising temperature (McGregor, 2017).

Thus, climate change and variability are the dominant phenomena in many countries and in particular for Ethiopia (Aragie, 2013). Moreover, the country faces a water resource impact to its surface water mainly river with highly supplied to irrigation that consumes more water than others (Panel & Climate, n.d.; Tadese et al., 2019). A major challenge to water resources management in Ethiopia is spatial and temporal variability, both primarily driven by climatic variability (ESCAP, 2017; Yalew et al., 2018). Hence, Awash river Basin faces a risk of extreme flooding and drought events, which can have severe adverse economic impacts (Yalew et al., 2018; Zilberman et al., 2003).

2.4 Hydrological extreme Simulation Modeling

Hydrological modeling is the process of mathematically representing the response of a catchment system (runoff) to precipitation events during the time period under consideration (Machiwal & Jha, 2012; EPA, 2017; ESCAP, 2017; Koutsoyiannis & Montanari, 2007b; Melsen, 2017; Pechlivanidis et al., 2017; Rind, 1991). It is a very effective tool in generating runoff forecast, based on weather forecast (Gao et al., 2016; Gautam & Consulting, 2014; Jenkins et al., 2019; Tessema, 2011). Moreover, hydrological models use climatic variables (e.g. precipitation, temperature, and evapotranspiration), catchment topography, and land use characteristics to simulate runoff (Devia et al., 2015; Eze & Kumahor, 2019; Flood & Tools, 2013; Shawul et al., 2019; Young et al., 2006).

Rainfall-runoff models are classified based on model input and parameters and the extent of physical principles applied in the model (Devia et al., 2015). Thus, hydrological model is an approximation of the complex reality using a system concept (Tessema, 2011). In both empirical and conceptual approaches measured hydrological variables, usually stream flow data, are needed for calibration in order to develop and parameterize the model (Weeink, 2010). Physically based models are based solidly on an understanding of the physical processes using fundamental hydrodynamic laws (Devia et al., 2015; Jenkins et al., 2019; Koutsoyiannis & Montanari, 2007; Tessema, 2011; Weeink, 2010). In the same way optimal ensemble threshold is also chosen to minimize the number of false alarms and misses, while optimizing the number of flood events correctly forecasted (Masia et al., 2018). Apart from forecasting and predicting models could also help in predicting the impacts of natural and

anthropogenic changes on water resources and also in quantifying the spatial and temporal availability of the resources (Kavetski et al., 2006; Prein, 2019; Y. P. Xu et al., 2010).

Hydrological models provide a sound physical basis for this purpose, and have the capability of simulating a wide range of flow situations (Beven & Beven, 2007; Beven & Binley, 2014; Khazaei & Ahmadi, 2013; L. Li et al., 2011). However, these models require accurate river geometric data, which may not be available at many locations. It is also not possible to integrate observed data directly at desired locations to improve model results (WMO, 2006; World Meteorological Organization, 2011b, 2011a). On the other hand, GIS-support for hydrological models is classified into the following levels: assessment, estimation of hydrological parameters, hydrological modeling, coupling of GIS and hydrological models (Giuliani et al., 2017).

Extreme hydrology can be simulated using complete rainfall-runoff models or using routing models (Hlavcova et al., 2005; Murphy, n.d.). The literature on flood simulation is full of examples of both types of models being used successfully for flood warning purposes (Flood & Tools, 2013; IPCC a, 2014; Martinez et al., 2010; WMO, 2018, 2019; World Meteorological Organization, 2020; World Meteorological Organization, 2013). Usually, routing methods-based flood simulation models are simpler and less data-intensive (Flood & Tools, 2013; Pachauri, 2014). Broad classifications of various model types falling under rainfall runoff models along with methods relying only on the routing to downstream of an observed wave (Physical & Basis, 2013). Similarly, digital elevation models have been applied to a distributed model for real-time prediction with a distributed basin simulator (Griffis & Stedinger, 2007; Koster et al., 2017; Li et al., 2012). However, models could be classified as hydrological, or hydraulic, according to (Flood & Tools, 2013). In practice, most extreme flow simulation use combination of rainfall-runoff and routing models (IPCC a, 2014; Lynch & Cassano, 2006; McGregor, 2017; Rind, 1991; World Meteorological Organization, 2013).

Similarly, Flood routing consists of attenuation and translation of flood hydrograph from upstream to downstream (EPA, 2017) and forecast using rainfall-runoff models (also called hydrological models), or routing models, or combination of both (Lynch & Cassano, 2006; WMO, 2018, 2019). Thus, precipitation is the activating signal of a hydrological process and stream flow is the part of precipitation that appears in a stream, and represents the total

response of a basin and consists of surface flow, subsurface flow, groundwater or base flow, and precipitation falling directly on the stream (ESCAP, 2017; Gautam & Dulal, 2013; Lynch & Cassano, 2006; Shah, 2017; Weeink, 2010; WMO, 2018, 2019).

Many advanced types of models exist, but they have been developed for a diverse range of climatic regions (Eumisd, 2015; Gao et al., 2016; Gautam & Consulting, 2014). Hence, these models must be adapted to the local situation of the study area prior to application. The ability to simulate river flow quickly and accurately is of crucial importance in flood forecasting operations (Gao et al., 2016; Jain et al., 2018; World Meteorological Organization, 2013). Moreover, hydrologic simulation employing computer models has advanced rapidly and computerized models have become essential tools for understanding human influences on river flows and designing ecologically sustainable water management approaches (World Meteorological Organization, 2013). Thus, hydrological models use physical detection systems to simulate extremes based on predicted or measured parameters (ESCAP, 2017; Melsen, 2017).

Models that provide a physically sound description about the hydrological processes that occur in a basin are expected to have significant advantages over purely empirical models (EPA, 2017). Hydrologic simulation models are used to provide a hydrologic prediction/projection as well as better understanding of processes within the hydrologic cycle (EPA, 2017; ESCAP, 2017; Keshta et al., 2019; Melsen, 2017; Meresa, 2019). A variety of modeling approaches are used for this purpose (Machiwal & Jha, 2012). These models are a simplified conceptual representation of a part/component of the global water cycle (Devia et al., 2015; Newman et al., 2021). Furthermore; simulation methods are able to represent the highly nonlinear processes of the water cycle (Belussi et al., 2007; Beven & Beven, 2007) and these models may deal with steady-state or transient conditions.

Different classifications are considered for hydrologic simulation. Two groups of hydrologic models are; Data-driven mathematical models: In these models, mathematical and statistical concepts are used to develop a relationship between model input(s) such as rainfall and temperature and model output such as runoff. The common procedures used in these models are regression, transfer functions, neural networks, fuzzy inference, and system identification (Daamen et al., 2003; Jenkins et al., 2019; Mockler et al., 2016). These models can be deterministic or stochastic and Physical (process)-based models: These models attempt to

simulate the physical processes that happen in the real world through the hydrological cycle based on identified physical and empirical relationships (Haining et al., 2010; McCuen, 2016; Mosavi et al., 2018; Rezaie-Balf et al., 2019). Typically, these models include representations of surface/ subsurface runoff formation, evapotranspiration, and channel flows/stream flows.

The physical-based hydrologic models of rainfall–runoff including lumped models, semi-distributed models, and distributed models with applications to HEC-HMS (Hydrologic Modeling System), IHACRES (acronym for Identification of unit Hydrographs and Component flows from Rainfall, Evaporation, and Stream flow data), Storm NET, and HBV (Hydrologiska Byråns Vattenbalansavdelning) are of types. HBV has been developed in the recent years, which is based on the conceptual estimation techniques (Seibert, 1997). This model becoming increasingly common in the analysis of hydrology and water resources problems (Eumisd, 2015; Gao et al., 2016; Gautam & Consulting, 2014). Thus, HBV model was developed from being a forecasting model to become a more general tool in many types of applications, whenever there is a need to transform meteorological observations into runoff and was the first operational applications (Bergström, 2006). Hence, Hydrological models are mainly classified into two main groups, physically-based and conceptual models (Beven, 2001).

2.4.1 Conceptual Models

Conceptual models were the first attempt to reproduce the different hydrological processes within a catchment in a numerical form (Davie, 2008). Rainfall is added to the catchment and a water budget approach used to track the losses (e.g. evaporation) and movements of water (e.g. to and from soil water storage) within the catchment area (EPA, 2017; Mehrotra, 2006). There are many examples in the literature of lumped conceptual models used to predict stream flows (Beven K. , 2001). The term ‘lumped’ is used because all of the processes operate at one spatial scale that is, they are lumped together and there is no spatial discretization and the scale chosen is often a catchment or sometimes sub-catchments (Skøien & Bl, 2006; Sood & Smakhtin, 2015a).

Conceptual models approximate key hydrological processes through simplified equations and lumped parameters that represent spatially averaged (Beven & Beven, 2007; Beven & Binley, 1992, 2014). The term ‘conceptual’ is used because the equations governing flow rates are often deemed to be conceptually similar to the physical processes operating (EPA, 2017). So,

the rate of flow through the catchment, and hence the estimated stream flow, is controlled by a series of parameters that need to be calibrated for a given catchment (Beven & Binley, 1992).

Calibration is normally carried out by comparing predicted flows to measured values and adjusting (or ‘optimizing’) the parameters until the best fit is obtained (EPA, 2017; Gao et al., 2016; Skøien & Bl, 2006). This technique obtains a similar predicted hydrograph using a completely different set of optimized parameters (Jin et al., 2010). Therefore, Lumped conceptual models offer a method of formulating the hydrological cycle into a water budget model that allows simulation of stream flow (Ajami et al., 2007; Almeida et al., 2006; Yen et al., 2018).

2.4.2 Physically based distributed models

The principle behind this type of model is that it is totally transparent; all processes operating within a catchment are simulated as a series of physical equations at points distributed throughout the catchment (Devia et al., 2015). In theory this should mean that no calibration of the model is required and spatially distributed model output for any parameter can be obtained (Jinkang et al., 2007; Machiwal & Jha, 2012; Pugliese et al., 2013). There are numerous problems associated with using a physically based, distributed model, as outlined by (Beven & Binley, 1992) and others. The primary problem is that the amount of data required to set the initial conditions and parameterize the model is vast (Emam et al., 2018; E M Mockler et al., 2016). However, the lack of data to run the model leads to spatial averaging of parameters (Dawson & Wilby, 2001; Islam, 2015b). Thus, there are also concerns with the size of grid used in applications (sometimes up to 1 km²) and whether it is feasible to use the governing equations at this scale (Bloschl & Sivapalan, 1995; Clark et al., 2017; Goovaerts, 2000; Kidd & Huffman, 2011). These types of problems led to query whether there really is such a thing as physically based distributed hydrological models or whether they are really just lumped conceptual models with fancier equations (Hengl, 2007; Islam, 2015a; Kampf & Burges, 2007; Yu et al., 2006).

The concept of physically based distributed hydrological modeling is noble, but in reality the models have not produced the results that might have been expected (Christakos et al., 2000; Lakshmi et al., 2001; Sood & Smakhtin, 2015b). However they have been useful for gaining a greater understanding of our knowledge base in hydrological processes. The approach

taken, with its lack of reliance on calibration, still offers the only way of investigating issues of land use change and predicting flows in ungaged catchments (Christakos et al., 2000; Haining et al., 2010; Song et al., 2015). The basis of the simulation techniques is the mathematical representation of hydrologic systems (Maidment, 1993). Due to the mathematical simplicity and flexibility of these techniques, they can be easily employed for analyzing the water cycle systems (Callow, 1994). Mathematical models, which are also called data-driven models, are used for evaluation of a system performance under a given set of inputs and operating conditions (Davie, 2008).

2.5 Uncertainty in hydrological extremes

The main source of hydrological model output value variability is the natural variability in hydrological and meteorological input series (UNESCO, 2005). Uncertainty is naturally quantified using probability theory in terms of probability distribution function (PDF)(Butts et al., 2004; Clark et al., 2017; Devia et al., 2015; Kidd & Huffman, 2011; Kusangaya et al., 2018; Vesely et al., 2019; Y. P. Xu et al., 2010) and the targeted uncertainty quantification should be no other than the quantification of the predictive uncertainty (Stott & Kettleborough, 2002).

Hydrological modeling uncertainty is traditionally recognized within the model calibration and validation phases (Andrés-Doménech et al., 2015). According to (Chen et al., 2013; Koster et al., 2017; Xu, 2014), an appropriate modeling approach for any uncertain hydrological system should necessarily include quantification of its uncertainty within a stochastic framework. Uncertainty quantification theories are subject to considerable and as better quantify accuracy and precision of model predictions (Keating, John, A., & Qinjun, 2010). Predictive hydrological uncertainty can be quantified by using ensemble methods (Papacharalampous, Tyralis, Koutsoyiannis, & Montanari, 2020). Perhaps the most frequently exploited methodology for predictive uncertainty quantification in hydrological modeling is the Generalized Likelihood Uncertainty Estimation (Beven & Binley, 2014). This approach has been proposed by (Beven K. , 1993; Beven & Freer, 2000), and is based on the concept of equifinality (Beven & Beven, 2007; Beven & Binley, 1992) . The quantification of uncertainty in the ensemble-based predictions of climate change and the corresponding hydrological impact is necessary for the development of robust climate adaptation plans (Younggu Her, Seung-Hwan Yoo, Cho, Syewoon Hwang, Jeong, & Seong, 2017).

2.5.1 Model parameters Uncertainty

The reliability of hydrological models is highly dependent on the calibration procedure, which is normally the search for one optimal parameter set (Seibert, 1997). Uncertainties in hydrological modeling includes associated with model inputs, model structure, parameter values and observed data (Sood & Smakhtin, 2015c). Thus, parameter uncertainty comes from priors on the mean and the variance terms of the logistic regression parameters, with a multivariate normal on the mean vector and inverse wish art on the covariance matrix(Clark et al., 2017; Machiwal & Jha, 2008; Wagener et al., 2001; Y. P. Xu et al., 2010). Accurate assessment of the parameters and predictive uncertainty of hydrologic models is an important aspect of any hydrologic modeling application (Schoups, Vrugt, Fenicia, & Giesen, 2010). Model parameter inferences are then based on a likelihood function quantifying the probability that the observed data were generated by a particular parameter set (Chowdhary & Singh, 2010). Accurate parameter uncertainty estimation is often required for regionalization and extrapolation of hydrologic parameters to ungagged basins (Vrugt, Gupta, Bouten, & Sorooshian, 2003). Another predictive uncertainty quantification methodology that has received attentions both by researchers and practitioners is the Bayesian Forecasting System (BFS) (Papacharalampous, Tyralis, Koutsoyiannis, & Montanari, 2020).

Uncertainty analysis is commonly based on a regression model, whereby observations are represented by the sum of a deterministic component and a random component describing remaining errors or residuals such as a functional form of the joint probability density function (pdf) of the residual errors (Devia et al., 2015; EPA, 2017; Kusangaya et al., 2018; McCuen, 2016; Sood & Smakhtin, 2015c; Xu et al., 2010). This statistical model is then used to derive the appropriate form for the likelihood function (Downer & Ogden, 2003; Jain et al., 2018). An advantage of the formal approach is that error model assumptions are stated explicitly, and their validity can be verified a posteriori (Stedinger et al., 2008). The uncertainty in results has to be analyzed in order to assess the reliability of the simulated variable and support the decision making process(Jain et al., 2018; Koster et al., 2017; Marton & Paseka, 2017; Song et al., 2015). However, the results of the model have to be evaluated, either by visually comparing observed and simulated plots by applying a mathematical criterion to calculate the distance between observed and simulated data(Xi Chen et al., 2013; Vrugt et al., 2008; A. Zhang et al., 2015). Both Visual and mathematical

evaluations may differ and generate different diagnosis on model quality and efficiency (Kavetski et al., 2006; Maity, 2018).

Several general approaches are available for estimating the parameters of a distribution (Beven & Binley, 2014; Butts et al., 2004; Jin et al., 2010; Kusangaya et al., 2018). Among many approaches the simple approach and mostly used one is the method of moments which uses the available sample to compute an estimate value of variable (Maity, 2018) ; so that the theoretical moments of the distribution of value exactly equal to the corresponding sample moments (Beven & Binley, 2014; Jin et al., 2010). Alternatively, parameters can be estimated using the statistical motivation is the method of maximum likelihood (Devia et al., 2015a; Jain et al., 2018; Koutsoyiannis & Montanari, 2007b; Melsen, 2017).

Moreover, the Maximum likelihood estimators (MLEs) have very good statistical properties in large samples, and experience has shown that they generally do well with records available in hydrology (Adeloye & Montaseri, 2002; Machiwal & Jha, 2008; Okali et al., 2019). However, often MLEs cannot be reduced to simple formulas, so estimates must be calculated using numerical methods (Griffis & Stedinger, 2007). Fitting a distribution to data sets provides a compact and smoothed representation of the frequency distribution revealed by the available data, and leads to a systematic procedure for extrapolation to frequencies beyond the range of the data set (Beven & Binley, 1992; Forestieri et al., 2016; Kiang et al., 2018; Kusangaya et al., 2018). When flood flows, low flows, rainfall, or water-quality variables are well-described by some family of distributions, a task for the hydrologist is to estimate the parameters of that distribution so that required quintile's and expectations can be calculated with the "fitted" model (Beven & Binley, 2014; Griffis & Stedinger, 2007; Koster et al., 2017; Meresa & Romanowicz, 2017; Mockler et al., 2016).

2.5.2 Estimating uncertainty propagation

Assessment of parameter and predictive uncertainty of hydrologic models is an essential part of any hydrologic study. Uncertainty analysis forms the basis for model comparison and selection (Schoups, Vrugt, Fenicia, & Giesen, 2010), allows identification of robust water management strategies that take account of prediction uncertainties (Hossain & Anagnostou, 2005). Estimation of parameter and predictive uncertainty of hydrologic models has traditionally relied on several simplifying assumptions. Residual errors are often assumed to

be independent and to be adequately described by a Gaussian probability distribution with a mean of zero and a constant variance (Schoups & Vrugt, 2010).

Moreover, Conceptual rainfall-runoff models have traditionally been applied without paying much attention to numerical errors induced by temporal integration of water balance dynamics (Zhou, et al., 2016). However, estimating parameter and predictive uncertainty using Markov chain Monte Carlo (MCMC) sampling is a powerful and flexible method (Schoups et al., 2010). These techniques are especially useful for the parameter inference of nonlinear hydrologic models (Smith, 1987). On the other hand, application to Bayesian uncertainty analysis of a conceptual rainfall-runoff model simultaneously identifies the hydrologic model parameters and the appropriate statistical distribution of the residual errors (Schoups and Vrugt , 2010). Therefore, the HBV model is calibrated by seeking one optimal parameter set that represents the catchment (Seibert, 1997). Similarly, there may be many sets of parameters which give similar good results during a calibration period, but their predictions may differ when simulating runoff in the future (Beirlant, Goegebeur, Teugels, Segers, Waal, & Ferro, 2004).

2.6 Extreme flow Analysis

2.6.1 Flood Frequency Analysis techniques

It is the application of statistical theory into an area that affects many people's lives, whether it is through flooding or low flows and drought (Beven & Binley, 1992; Devia et al., 2015; EPA, 2017; Jain et al., 2018). Annual maximum series (AMS) approach in hydrologic frequency modeling, the partial duration series (PDS) method, also denoted the peaks over threshold (POT) method, has been advocated (Madsen, Pearson, & Rosbjerg, 1997). The analysis of how often an event is likely to occur is an important concept in hydrology (Devia et al., 2015). The techniques that mainly emphasis on flood frequency analysis to attempt a probability on the likelihood of a certain event occurring (Devia et al., 2015a; Koutsoyiannis & Montanari, 2007b; Machiwal & Jha, 2008; Okali et al.,2019; Pechlivanidis et al., 2017). Predominantly it is concerned with the low-frequency, high-magnitude events with large flood or a very low river flow (Adeloye & Montaseri, 2002; Okoli et al.,2019). Thus it is important to differentiate between the uses of flow duration curves and frequency analysis methods (Beven & Binley, 1992; Karakoram, 2016). Hence, flow duration curves tell us the

percentage of time that a flow is above or below a certain level and the average data that describes the overall flow regime (EPA, 2017; Mason et al., 2015).

Flood frequency analysis is concerned only with peak flows: the probability of a certain flood recurring (EPA, 2017; ESCAP, 2017; Jain et al., 2018). Conversely, low flow frequency analysis is concerned purely with the lowest flows and the probability of them recurring (Beven & Binley, 1992). Thus, flood frequency analysis is probably the most important hydrological technique and the concept of a '100-year flood', or a fifty-year recurrence interval, concerned with peak flows (EPA, 2017; Beven & Binley, 2014). There are two different ways that a peak flow can be defined: • the single maximum peak within a year of record giving an annual maximum series; or • any flow above a certain threshold value, giving a partial duration series (Beven & Binley, 1992, 2014). Therefore, Hydrologic hazard curves and flood hydrographs are used to evaluate hydrologic risks for a given facility (Newman et al., 2021). Hence, a hydrologic hazard curve is a curve that relates probability of occurrence to magnitude of a flood (Newman et al., 2021).

There are numerous approaches to developing these curves, including (1) Statistical stream gauge analysis, e.g., calculating the annual exceedance probability (AEP) (Newman et al., 2021); (2) 'Design storm' rainfall-runoff hydrologic model estimates, where the return period of the flood is equal to the return period of the precipitation (Newman et al., 2021); and (3) Fully stochastic rainfall-runoff modeling to explicitly represent the impacts of hydrological processes on floods (Newman et al., 2021). Flood frequency analysis is to describe the statistical properties of the distribution of flood events and to estimate design flood values for a desired return period (Cunderlik et al., 2013). And applied to maximum (usually annual maximum or peaks-over threshold) values of instantaneous or mean daily stream flow series (Cunderlik et al., 2013). Flood-duration-frequency modeling is an extension of standard flood frequency analysis that takes into account the multi-duration aspect of flood hydrographs (Cunderlik et al., 2013). The interpretation of flow duration curve shape discussed so far is essentially subjective (Beven & Binley, 1992; Butts et al., 2004; EPA, 2017; ESCAP, 2017; Forestieri et al., 2016; Jain et al., 2018; Kiang et al., 2018; L. Li et al., 2011; Marton & Paseka, 2017) and the statistics derived from the curve; the three most important ones are:

- The flow value that is exceeded 95 per cent of the time (Q95). It is useful statistic for low flow analysis.

- The flow value that is exceeded 50 per cent of the time (Q50). This is the median flow value.
- The flow value that is exceeded 10 per cent of the time (Q10) and useful statistic for analysis of high flows and flooding.

In flood frequency analysis there are three interrelated terms of interest. These terms are interrelated mathematically, the probability of exceedence: $P(X)$. This is the probability that a flow (Q) is greater than, or equal to a value X . The probability is normally expressed as a unitary percentage (i.e. on a scale between 0 and 1). The relative frequency: $F(X)$. This is the probability of the flow (Q) being less than a value X . This is also expressed as a unitary percentage. The average recurrence interval: $T(X)$. This is sometimes referred to as the return period. $T(X)$ is a statistical term meaning the chance of expedience once every T years over a long record (Beven & Binley, 1992; Butts et al., 2004; Kiang et al., 2018).

2.7 Extreme frequency Probability distribution models

Probability distribution models are applied in extreme flood analysis, drought investigations, reservoir volumes studies, and time-series modeling, among other various hydrological studies (Cunderlik, Jourdain, Ouarda, & Bobée, 2007). However, the selection of the most suitable probability distribution and associated parameter estimation procedure in flood frequency analysis has remained the most difficult task for many researchers (Langat, Kumar, & Koech, 2019). Several probability distribution functions have been developed to fit the sample distributions (Devia et al., 2015; Koster et al., 2017; Nile et al., 2020). The suitability of the candidate probability distributions can be evaluated by considering their ability to reproduce different features of the annual maximum flow series (upper bound of the distribution, upper tail of the distribution, the shape of the body of the distribution, lower tail of the distribution, lower bound of the distribution) that are of particular importance in flood frequency modeling (Belussi et al., 2007; Burgan & Aksoy, 2020; Mockler et al., 2016; Nile et al., 2020; Prudhomme & Reed, 1999; Zhang, & Zhou, 2016; Romali & Yusop, 2017; Xu et al., 2010b).

Extreme precipitation with a certain return level is typically estimated using extreme value analysis under a stationary climate assumption (Nakaegawa, Kobashi, & Kamahori, 2020)(Nakaegawa, Kobashi, & Kamahori, 2020). In formulating a flood control plan, that is,

a high-water plan, precipitation with the same return level as the designed flood is used according to the theorem of extreme value analysis (Nakaegawa, Kobashi, & Kamahori, 2020); Koster et al., 2017; Xu et al., 2010b, 2010a). On the other way a parametric approach, the designed precipitation is estimated using parametric extreme value distributions, but its magnitude varies with the selection of extreme value distribution and the treatment of outliers ((Nakaegawa, Kobashi, & Kamahori, 2020); Griffis & Stedinger, 2007; Hlavcova et al., 2005).

The use of probabilistic approaches to fit and select the best fitting probability model to a set of observed data has lately gained currency among researchers (Xi Chen et al., 2013; Devia et al., 2015b; Meresa & Romanowicz, 2017; Sood & Smakhtin, 2015a; Sun et al., 2017; Xu et al., 2010a). Moreover to describe the flood frequency at a particular site, the choice of an appropriate probability distribution and parameter estimation method are of immense importance (Romali & Yusop, 2017).The probability distributions used in this study was include the generalized extreme value (GEV) distribution, Pearson type-III (P3) distribution, Gumbel (GUM) distribution and three-parameter log-normal (LN3) distribution (Ul et al., 2019).

The choice of a model follows a procedure with a number of steps, starting with the critical analysis of historical data, the selection of an event-descriptive variable to examine the magnitude of a flood, and finally, evaluating the adequacy between a flood sample and a distribution type to inform the selection (Beven & Binley, 1992, 2014; Xi Chen et al., 2013; Forestieri et al., 2016; Khazaei & Ahmadi, 2013; Kiang et al., 2018; Li et al., 2011; Mockler et al., 2016; Yen et al., 2018). Among several distribution families the commonly used in hydrological extreme includes the normal/lognormal family, the Gumbel/Weibul, generalized extreme value family, and the exponential/Pearson/log-Pearson type III family (Bruin & Trigo, 2019; Devia et al., 2015; Nile et al., 2020; Sood & Smakhtin, 2015a). Mostly probability distribution models viz., Weibul, gamma (Pearson type 3), Generalized extreme value (GEV), lognormal, Gumbel, and normal are in use in the hydrologic frequency analysis of floods (Her et al., 2019; Jain et al., 2018; Kiang et al., 2018; Koster et al., 2017; Koutsoyiannis & Montanari, 2007b; Mockler et al., 2016; Okali et al., 2019; Pechlivanidis et al., 2017).

Generalized extreme value is a continuous probability distribution developed within extreme value theory (Samantaray & Sahoo, 2020). It is utilized as an estimate for modeling maxima of lengthy (limited) series of arbitrary variables. Significantly, while using this distribution, the upper bound is unidentified and hence has to be projected; when Weibull is applied, the lower bound is identified as zero (Koutsoyiannis & Montanari, 2007b; Melsen, 2017; Norman et al., 2019; Sun et al., 2017; Weeink, 2010; Xu et al., 2010a). On the other hand, Log Pearson III is a statistical method of fitting frequency distribution values for predicting flood at a few sites of a specified river (Xi Chen et al., 2013; Xu, 2014). So that a frequency distribution is built after calculating data related to statistics at a particular river site (Meresa & Romanowicz, 2017; Sun et al., 2017; Wu et al., 2011). On the other hand flood occurrence probability of different densities can be taken out from the curve (H.K. Meresa & Romanowicz, 2017; Song et al., 2015; Sun et al., 2017; Wu et al., 2011; Y. P. Xu et al., 2010). This particular method helps in extrapolating event data with return periods ahead of pragmatic occurrence of flood (Y. P. Xu et al., 2010). Thus, after finding the actual discharge, the calculated natural logarithm of the actual discharges (Z) and the standard logarithmic mean (μ) and standard logarithmic deviation (σ) of the calculated discharges for the respective seasons will be determined (Cunderlik et al., 2013; L. A. Melsen, 2017; Newman et al., 2021; Norman et al., 2019; Sun et al., 2017; Weeink, 2010; Y. P. Xu et al., 2010)

3. STUDY AREA DESCRIPTION

3.1 Location

The study area was located between $70^{\circ} 53' 42''$ to $120^{\circ} 07' 20''$ North and $370^{\circ} 56' 56''$ to $430^{\circ} 17' 04''$ east. Awash River Basin originates near Ginchi in the central highlands of Ethiopia, and flows north east through the northern section of the Rift Valley to eventually discharging into Lake Abbe near Djibouti boarder, traveling a distance of about 1200km with a total catchment area of 116,000 square kilometers. Considering hydrological, administrative, economic and social situations the Basin sub divided into six sub basin catchments (Figure 1), namely, Awash Upstream Koka, Awash Awash, Awash Halidebi, Awash Adaitu, Awash Terminal and Eastern sub basin. Awash US Koka sub basin comprises Awash Kuntre River, Mojo River and Akaki River.

Moreover, the Upper Awash catchment is found in the highlands of central Ethiopia with all lands above 1500 masl. The land use condition in the Upper Awash catchment includes mainly of cultivated agricultural land, forest land. The Upper Awash River covers the river section from its source up to Koka Reservoir. The Upper Awash River drains a catchment area close to $11,300 \text{ km}^2$ and the length of the river up to Koka is around 220 km (Halcrow, 1989; Profile, 2019). Therefore, this study was conducted at three sub catchments , namely Akaki, Melka Kunture and Up stream of Koka in Upper Awash River Basin(Figure 1).

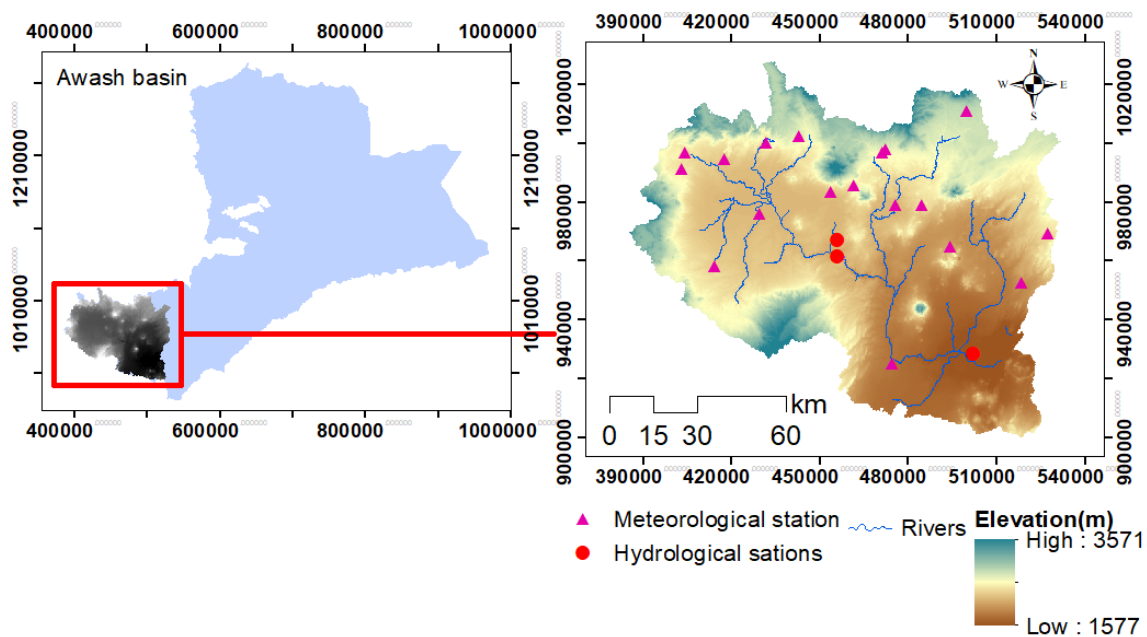


Figure 1. Location and map of Upper Awash River Basin

3.2 Land Use and Land Cover

The Awash basin is the most developed area with more than 60% of the potential irrigable area has been developed (Kerim et al., 2016). The land use/cover (LULC) of Upper Awash Basin consists mainly of cultivated agricultural land, grass land and shrub land, which cover 93.2% of the total area; about 3.6% is covered by savanna and the remaining 3.2% comes from the other land cover types. Upper Awash Basin LULC covers agriculture, bare land, urban and shrub land, forest, grassland, water, and wetland (Profile, 2019). LULC Changes from 1986 to 2009 under agriculture is 39.55 %, forest 42.76 %, urban 0.73 % and bare land 0.13 % from the watershed.

3.3 Climate

The basin receives 100 – 1700mm mean annual rainfall with its wide spatial and temporal variation. According to the annual water balance the basin generate 10.3BCM water for ground water recharge, 4.6BCM water as stream flow, and 3.6BCM water as stored in open water systems that include lakes, reservoirs and wetlands of the basin. Therefore the water potential of the basin can be accounted as 8.2BCM surface water potential and 10.3BCM ground water potential with 300m exploration (Awash water assessment report, 2010). It is obvious these water resources potential has temporal and spatial variation over the basin. Particularly, its temporal variation with 71% and 29% share for rainy season (June –October) and dry season (November – May) respectively has significance important to direct the water resources development of the basin to focus on water harvesting and storage structures.

The mean annual rainfall varies from about 1600 mm at Ankober, in the highlands north east of Addis Ababa to 160 mm at Asayita on the northern limit of the Awash River Basin. Addis Ababa receives 90% of its annual rainfall during the rainy period March to September. At Dubti the same overall proportion is received during the two rainy periods, distributed 30% and 60% respectively. The mean annual rainfall over the entire Western Catchment is 850 mm and over the headwaters of the Awash, as gauged at Melka Hombole it is 1216 mm. Over the Eastern Catchment the mean annual rainfall is estimated to be 456 mm. The annual and monthly rainfalls are characterized by high variability.

The Upper Awash watershed was found in the high lands of central Ethiopia above 1500 m above mean sea level. In the Upper Awash watershed, there are two rainy seasons (bi-modal

rainfall patterns) such as heavy rainfall from Jun-August and low rainfall from March-April. The watersheds receive its maximum rainfall during June to September (70 % to 75 % of the annual rainfall). The second rainy period covers the period from February to May. The highest records are observed in July and August whereas the lowest records are observed in November and December. The annual rainfall varies from 650 mm to 1600 mm. The average annual temperature pattern of weather generator station which varies from 16.07 to 17.29 °C (Profile, 2019).

3.4 study areas characteristics and input datasets

To avoid the human intervention effect on flow prediction, three medium-sized natural river catchments (unregulated and unurbanized) were selected to estimate uncertainty propagation from input to frequencies of hydrological extremes simulation. These three river basins were located in different hydro-climatic and physiographic conditions: namely, Akaki, MelkaKunture, and Upstream Koka catchments (Figure 2). The selected case study catchments vary in the climate regime, drainage density, river length, catchment area and shape, topography, soil type, surface and subsurface properties, land use, and land cover type. The hydro climatic properties of these three catchments are summarized in Table 1, of the selected catchments, low flow varies from 0.91 (MelkaKunture) to 3.21 m³/s (Akaki). This may happen and is commonly seen in ephemeral rivers. The selected catchments' drainage area ranges from 1475km² (Akaki) to 7093km² (Upstream Koka).

Table 1. The statistical description of observed stream flow and precipitation in 1981-2010.

Gauge Station	Latitude [degree]	Longitude [degree]	Area [km ²]	Q ₅ [m ³ /s]	Q ₉₅ [m ³ /s]	Precipitation mean [mm]
MelkaKunture	8.7	38.6	4456	0.91	148.92	3
Akaki	8.75	38.6	1475.8	3.21	222.01	2.9
U/S Koka	8.4	39.02	7093.9	2.05	426.34	2.6

Similarly, the catchments are in different geographical locations (Figure 2). The observed precipitation, temperature, and stream flow data were collected from the Ethiopian Meteorological Agency, Awash River Basin Authority and Ethiopia's Water, Irrigation and Electricity Ministry. The length and quality of the available meteorological and hydrological

records are good; 30 years of recorded data from 1981 to 2010, from which the first 20 years (1982-2001) recorded data was used for calibration, and the remaining nine years (2002-2010) recorded data validation of the hydrological model. Daily potential evapotranspiration was estimated by using a temperature-based technique (Hamon, 1963).

4. METHODOLOGY

4.1 Modeling and numerical Techniques Design

Uncertainty propagation from the input data quality (precipitation and temperature) to the extreme hydrological signatures was conducted using a combination of the HBV hydrological model (Bergstrom, 1976), three distribution models (Log-Normal, Pearson-III, and GEV), and 20,000 HBV hydrological parameter sets (Figure 3). The 1,000 generated precipitation and temperature time series using a statistical approach were used for input data uncertainty band estimation. The 20,000 realizations of hydrological simulations using MCS-GLUE were applied for hydrological parameter uncertainty band estimation (Beven & Binley, 1992). Finally, three different frequency distribution models to estimate peak and low flow simulations were applied (Figure 3).

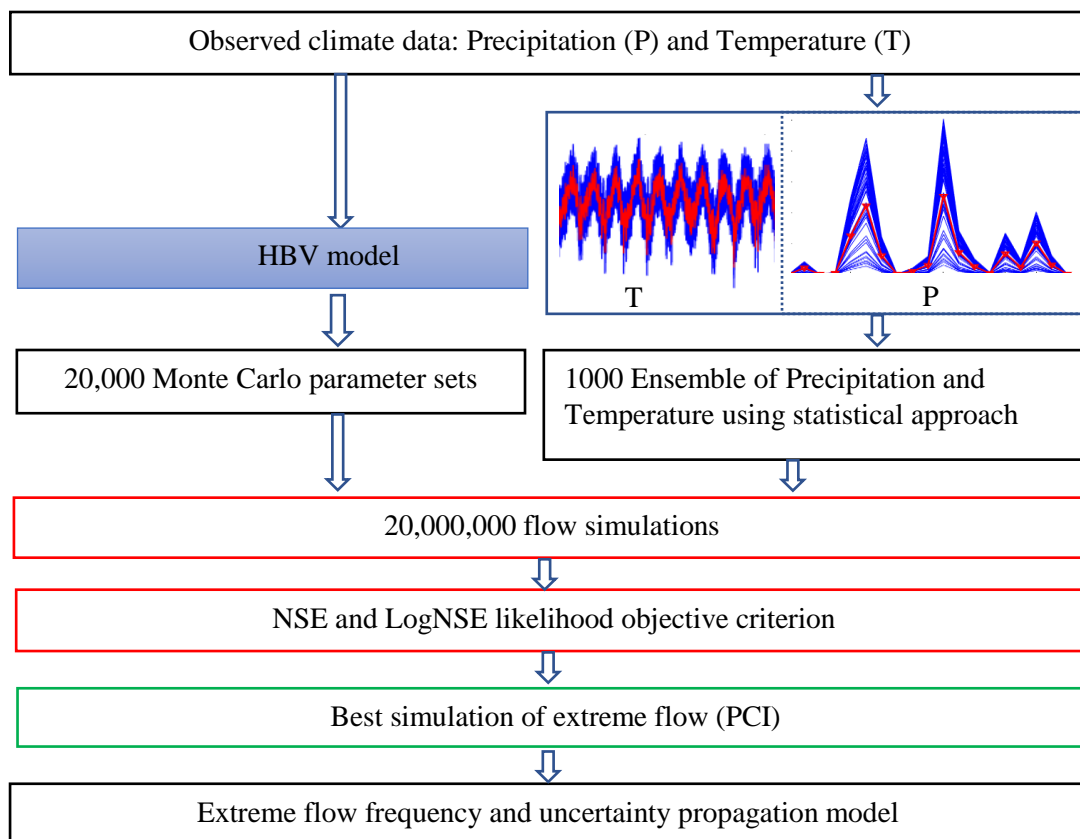


Figure 2. Designed computational flow chart of the research

4.2 Input data ensemble generation and modeling: Precipitation and temperature

Climate variables play a key role in the hydrological process and are highly varied and sensitive overtime and space (WMO, 2018). Of which, temperature and precipitation are associated with the pattern of regional and local atmospheric circulations (Kidd and Huffman, 2011; Mockler et al., 2016). In recent decades, various advanced statistical and stochastic approaches have been developed for climate predictions by incorporating the seasonal and annual fluctuations (Wu et al., 2011; Khazaei and Ahmadi, 2013; Breinl et al., 2017). These studies were highly exposed to uncertainty due to the complex stochastic approach (Vesely et al., 2019) and a number of parameters (Breinl et al., 2017; Okali et al., 2019).

The ensemble realization of precipitation and temperature were generated using a statistical approach (equation (1) and equation (2)) for assessing the input data uncertainty. Monte Carlo simulation with Gaussian distribution sampling was used to sample 1000 precipitation and temperature ensemble of realizations by multiplying (due to higher seasonal variability) and adding (lower seasonal variability) noise term $EPE_{j,n}$, and $ETE_{j,n}$, to observed precipitation and temperature recorded data, respectively (Ajami et al., 2007). The observed climate variables are perturbed at a given time by the error terms derived from the Gaussian distribution with constant mean and standard deviation, $N(0.01, \sigma_p^2)$ and $N(\mu_t, \sigma_t^2)$ for precipitation and temperature, respectively. Here the constant mean that used for ensemble precipitation was use as 0.01 because when I used the constant mean the result was given the same result as ensemble temperature error so, to get too much value I used 0.01 that is to reach up to 100% confidence. The statistical approach introduced in this study for generation of ensemble precipitation and temperature mentioned as follows:

$$PPE_{n,j} = PPO_n * EPE_{n,j}; \text{ where } EPE_{n,j} \approx N(0.01, \sigma_p^2) \quad \text{Equation 1}$$

$$TTE_{n,j} = TTO_n + ETE_{n,j}; \text{ where } ETE_{n,j} \approx N(\mu_t, \sigma_t^2) \quad \text{Equation 2}$$

Where n represents a simulation at a specific time and j denotes the j^{th} ensemble of realizations. $PPE_{n,j}$, and $TTE_{n,j}$ represent the number of an ensemble of precipitation and temperature realization at time n , respectively. TTO_n and PPO_n symbolize the observed precipitation and temperature at time n , respectively. The $EPE_{n,j}$ and $ETE_{n,j}$ represent the possible ensemble of errors variability range of generated precipitation and temperature at time n , respectively.

4.3 Hydrological extreme modeling

Hydrological model employed in a particular application depends largely upon the primary processes that produce runoff and their spatial and temporal extent, spatial coverage and resolution of data, and catchment features (Eumisd, 2015; Gao et al., 2016; Kauffeldt et al., 2016). Hydrological models, which mimic the natural hydrological processes based on conceptual, physical and/or empirical laws, have played important roles in modern flood forecasting (Eumisd, 2015; Gao et al., 2016; Kauffeldt et al., 2016).

4.3.1. Conceptual modeling

Conceptual models interpret runoff processes by connecting simplified components in the overall hydrological process (Shah, 2017). They are based on reservoir storages and simplified equations of the physical hydrological process, which provide a conceptual idea of the behaviors in a catchment (EPA, 2017). Therefore, conceptual models represent the water balance equation with the conversion of rainfall to runoff, evapotranspiration, and groundwater (EPA, 2017; McCuen, 2016). Each component in the water balance equation was estimated by mathematical equations that distribute the precipitation input data. The general governing equations for conceptual models are versions of the water balance equation which control surface water and storage fluctuations shown below in Equation (3) (EPA, 2017; ESCAP, 2017; McCuen, 2016).

$$\frac{dS}{dt} = P + ET + Q_s - G_w \quad \text{Equation 3}$$

Where dS/dt is the change in reservoir storage, P is precipitation, ET is evapotranspiration, Q_s is surface runoff, and G_w is groundwater.

Flood simulation using HBV hydrological model have been widely applied to flood forecasting for decades (Basins & Kan, n.d.; Gao et al., 2016). Hydrological phenomena are extremely complex, highly non-linear, and exhibit a high degree of spatial and temporal

variability (Jenkins et al., 2019) and estimate of the future state of some phenomenon such as flow rate, cumulative volume, stage level, and area of inundation or mean flow velocity at a particular geographical location or channel section (Flood & Tools, 2013). Therefore, HBV was mainly designed to simulate stream flow using precipitation, temperature, and evapotranspiration (Bergstrom, 1976). Catchment forest status and elevation of precipitation station (or centroid elevation) were also used.

The hydrological modeling Hydrologiska Byråns Vattenbalansavdelning (HBV) applied in this study was performed to predict continuous precipitation on daily time step (Bergström, 2006). The HBV was widely applied in different hydro-climate condition of the world (Meresa et al., 2017; Meresa and Gatachew, 2018; He et al., 2018b ; Neural & Ann, 2018). The HBV hydrological model was processed based conceptual model with parameters collected directly from field data (stream flow). Input parameters were calculated from the existing climatic and physiographic characteristics of the catchment. Hence, the HBV was implemented on the Upper Awash River Basin for Akaki, Melka Kunture and Upstream Koka with input data (precipitation and temperature) 30 years period was used and calibrated against field data of stream flow from 1981 to 2010. Input variables to the HBV model were used normally 24-hourly values of precipitation and air temperature and potential evapotranspiration was computed by Hamon formula. Finally, nine parameters were selected to control the input and output catchment process (Table 2).

Table 2. Range of hydrological parameters of HBV model and L stands for Lower value and U for the Upper part of the model parameters

parameter	Description	HBV L	HBV U
FC	Field capacity	0.1	250
BETA	Shape coefficient	0.01	5
LP	threshold for reduction of evaporation	0.1	2
ALPHA	measure for non-linearity of snow in quick runoff	0.1	0.6
KF	recession coefficient for runoff from quick runoff	0.005	0.6
KS	recession coefficient for runoff from base flow	0.005	0.6
PERC	percolation rate occurring when water is available	0.01	400
CFLUX	rate of capillary rise	0.5	400
WHC	water holding capacity	0.1	2.1

4.3.2 Hydrological model parameter evaluation

Most hydrological models need calibration to perform well (Beven & Binley, 2014; EPA, 2017; Jain et al., 2018; Meresa & Romanowicz, 2017). But the calibration option is not always there and today at least three situations can be identified with reference to the calibration and application of hydrological models (Bergström, 2006). Model datasets were divided into calibration and validation datasets (Kavetski et al., 2006; Meresa & Romanowicz, 2017; Xu et al., 2010). Hence, an optimum values of parameters were identified for the calibration dataset by minimizing the difference between observed and computed discharges (Song et al., 2015; Xu et al., 2010). Model performance was then tested for the validation dataset (Song et al., 2015; Xu et al., 2010; Yen et al., 2018). Thus, graphical plots and numerical measures has been evaluated for calibration and validation datasets: such as Joint plots of observed and computed hydrograph, and Percent bias (relative bias), or mean percent error (Devia et al., 2015; ESCAP, 2017; Koutsoyiannis & Montanari, 2007). Therefore, visual inspection of simple plots (hydrograph, scatter plot) that compared the predictions to actual measurements in calibration and validation dataset was provided significant information about how much the predictions were close to the observations, for different flow regimes (EPA, 2017; ESCAP, 2017).

Many different ways of parameter sampling from the upper and lower boundary of hydrological parameters, which depend on the computing times and number of parameters in a specific hydrological model developed (Machiwal & Jha, 2008; Okoli et al., 2019). Beven and Binley, (2014) stated that there is no fixed threshold in parameter sampling that varies from thousand to hundred thousand parameter sets. In this study, two objective functions were used to simulate both flow regimes (high and low flow regimes) and evaluated against observed stream flow (Machiwal & Jha, 2008). NSE, Equation (4) objective function was for high flow simulation and LogNSE Equation (5) for low flow simulation (Beven & Binley, 2014). Based on each model's performance, 200 sets of simulations for each hydrological model and data input were selected as a behavioral condition.

$$NSE = 1 - \frac{\sum_{t=1}^j (Q_{o,t} - Q_{m,t})^2}{\sum_{t=1}^j (Q_{o,t} - \bar{Q}_o)^2} \quad \text{Equation 4}$$

$$\text{LogNSE} = 1 - \frac{\sum_{t=1}^j (\log(Q_{o,t}) - \log(Q_{m,t}))^2}{\sum_{t=1}^j (\log(Q_{o,t}) - \overline{\log(Q_{o,t})})^2} \quad \text{Equation 5}$$

where $Q_{o,t}$, and $Q_{m,t}$ is observed and simulated flow at time t , Q_o is the mean observed flow, and j is the length of the time series. For each hydrologic model, the best values of NSE and LogNSE are selected for hydrological model structure and parameter uncertainty analyses.

4.4 Evaluation of ensemble simulations

Simulations' ensemble was evaluated using the proportion of extreme flow inside 95% confidence intervals (PCI) principle. Two hydrological extremes, peak, and low flow were used and evaluated by the derived CI. This is very helpful to identify (fix threshold) the behavioral and non-behavioral simulations and select the best threshold value of NSE and LogNSE. According to Li et al. (2011) and Xu, (2014), PCI way of ensemble evaluation is more reliable and efficient in uncertainty analysis. Zero flows were commonly observed in the low flow analysis and handled by setting the lower boundary of PCI with zero, whereas the upper part of the PCI is calculated using equation (6).

$$PCI = \left[1 - \left| \left(\frac{NQ_{i,p}}{T} - 0.95 \right) \right| \right] * \frac{1}{T} * \left[\left(\sum \frac{L_{u,t,p} - L_{l,t,p}}{Q_{o,T}} \right) \right] \quad \text{Equation 6}$$

where $L_{L,t,p}$ and $L_{U,t,p}$ are the lower and upper boundary values of the extreme flow at time t and portion p , T is the sum of time steps, $Q_{o,t}$ is the observed extreme flow at t time step, $NQ_{in,p}$ is the number of extreme flow observations which lie within the extreme flow CI. The PCI is used in 95% CI evaluation, which ranges from zero to infinity values (L. Li et al., 2011). The shape of the 95% CI is governed by PCI's weight; if PCI is closer to 0.95, it means more of the observed time series extreme fall in the confidence interval band.

4.5 Extreme Frequency Analysis (EFA)

Extreme frequency analysis is crucial to understand the probability of floods and/or low flows, and various distributions have been used to estimate these frequencies. A single distribution model may not be able to capture the entire temporal and spatial variability of hydrological extremes. Therefore, in extreme frequency uncertainty analysis, three common distribution types (Log-Normal, Pearson-III, and GEV) were extensively applied worldwide in extreme frequency modeling (Griffis and Stedinger, 2007; Madsen et al., 2013; Chen et al.,

2013). These distributions were fitted to extreme low and high flow to understand hydrological flood and low flow in the selected three catchments. In equations (7)-(9), the respective probability density function (PDF) of each distribution is presented. The exponential distribution was a simple model with one parameter, whereas Log Normal and Gamma had two parameters and whereas GEV had three parameters. In this research, one-two-three parameter distributions were considered.

$$\text{Log-Normal} \quad f(x) = \frac{\exp\left(-\frac{1}{2}\left(\frac{\ln x - \mu}{\sigma}\right)^2\right)}{x\sigma\sqrt{2\pi}} \quad \sigma, \mu (\sigma > 0) \quad \text{Equation 7}$$

$$\text{Pearson-III} \quad f(x) = \frac{(x-\gamma)^{\alpha-1}}{\beta^\alpha \Gamma(\alpha)} \exp\left(-\frac{x-\gamma}{\beta}\right) \quad \alpha, \beta, \gamma (\alpha > 0, \beta > 0) \quad \text{Equation 8}$$

$$\text{GEV} \quad f(x) = \begin{cases} \frac{1}{\sigma} \exp\left(-\left(1 + kz\right)^{-\frac{1}{k}}\right) \left(1 + kz\right)^{-1-\frac{1}{k}} & k \neq 0 \\ \frac{1}{\sigma} \exp(-z - \exp(-z)) & k = 0 \end{cases} \quad K, \sigma, \mu (\sigma > 0)$$

Equation 9

4.5.1 Generalize Likelihood Uncertainty Estimation (GLUE)

GLUE is a non-formal statistical approach that includes Monte Carlo simulations. The hydrological model runs using the entire space of hydrological parameter combination sets were evaluated by deploying the goodness-of-fit criterion (Beven, 2007). A likelihood function $Z(X)$ was used to separate the non-behavioral and behavioral simulations produced by different variables X . Every i^{th} of the variable X had its own one likelihood measure at time t . The ensemble of each variable X_i ($i=1, \dots, m$) provides the multi-likelihood measure values $Z(X_i)$. The GLUE function shown in Equation (10), where the standard deviation/variance of residual σ_e^2 values was the variance of error in the estimated results affected by the model parameters. If the estimated value of σ_e^2 is near equal to the estimated maximum likelihood or equal to the standard deviation/variance of the observation data σ_o^2 , the likelihood measure $Z(X)$ is equal to zero, which indicates extremely high uncertainty.

$$\mathbf{Z}(\mathbf{X}) = \mathbf{1} - \frac{\sigma_0^2}{\sigma_e^2} \quad \text{Equation 10}$$

4.5.2 Uncertainty decomposition

Analysis of variances decomposition (ANOVA) can decompose the aggregated source of uncertainty into individual terms and their interactions (Meresa & Romanowicz, 2017). In this study, one-way ANOVA Equation (11) was used to distinguish the main variable effects and their interaction effect on the aggregated extreme frequency indices.

$$\mathbf{SST} = \mathbf{SS}_{ID} + \mathbf{SS}_{HP} + \mathbf{SS}_{IDHP} + \mathbf{Error} \quad \text{Equation 11}$$

Where SST is the square sum of the total error, SSID is the sum of the standard error of input data, SSHP stands for sum standard error of hydrological parameters, and SSIDHP is the sum of standard errors of the combined effect of input data and hydrological parameters and total sum fitting Error.

5. RESULTS

4.1 Ensemble of input precipitation and temperature evaluation

Figure 4 evaluates the ensembles precipitation and temperature time series data with 95% confidence interval, respectively. The highest 1000 coefficient of determination (RR) values and their respective time series of daily precipitation and daily air temperature (Figure 4) were selected for further use in forcing a hydrological model and assess the input uncertainty. The generated ensemble of precipitation and temperature has shown a very high correlation, and the observed values are fall in 95% of the confidence interval. In fact, 95% confidence interval (CI) of the 100 groups of generated precipitation is much more highly correlated to observed data than the total ensembles. This indicates that the proposed statistical climate generator approach performs well in generating an ensemble of precipitation and temperature and capturing the annual dynamics and variability of the climate variables. Interestingly, the spread of the peak precipitations of Akaki, MelkaKunture, and U/S Koka catchments are significantly wider. It may have a clear impact on the uncertainty band of extreme flow (Figure 4). Meanwhile, the spread of temperature values is not significantly changed within the sample (Figure 4). The RR values range from 0.7 to 0.98 and have a lower percentage of variance with observed time series. This implies that precipitation has relatively higher variability in magnitude and intensity, while the temperature does not significantly vary in the given period.

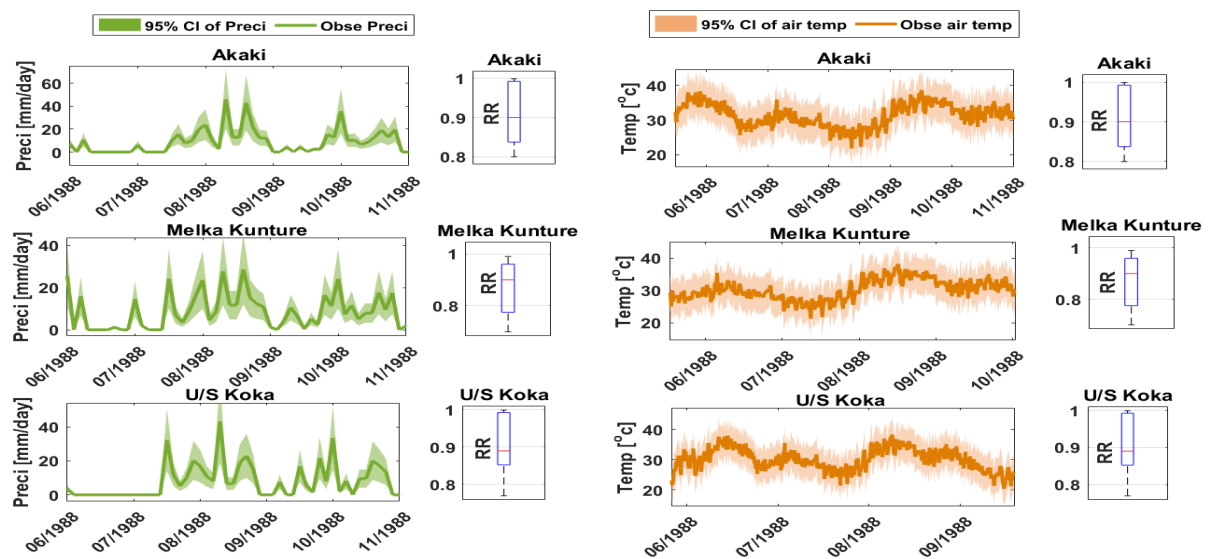


Figure 3. The confidence band of the highest 1000 generated precipitation time series with a respective boxplot of the coefficient of determination (RR). The green shaded area is a 95% CI of daily precipitation (preci), and orange is for daily air temperature (Temp).

4.2 Calibration and Validation of Hydrological model

To ultimately capture the extreme stream flow predictions, two objective functions were used. The NSE for extreme high stream flow prediction and LogNSE for extreme low flow were used to separate the most behavioral parameter sets from the lower one. Figure 8 presents the bounded NSE and LogNSE values that result from the best 100 hydrological parameter sets using the HBV model and their respective weights. The LogNSE and NSE results show not one-to-one related groups and had not significant correlation. This confirms that different hydrological parameter values govern each hydrological regime. The median of each objective function for each catchment using HBV hydrological model was quite good and promising for uncertainty estimation. For example, Akaki, MelkaKunture, and U/S Koki's NSE values are 0.8, 0.73, and 0.76, respectively (Figure 5). Also, the best NSE and LogNSE values were further used for hydrological parameter uncertainty investigation.

Overall, Figure 8 shows the hydrological model performance results using MC sampling with GLUE and bounded NSE and LogNSE objective functions for each catchment. The bounded likelihood function has more advantages to compare the results of hydrological models (Mathevet et al., 2006). Unlike, the NSE (one side bounded objective function) has fixed upper and lower boundaries $[-1 \ 1]$. The HBV hydrological model performed reasonably well to simulate river flow. However, the extreme flow simulation is challenging and had a very wide range of NSE values. The mean NSE and LogNSE value of each catchment show a reasonably acceptable value and feasibility to understand the catchments' uncertainty, keeping the varying results between them. The uniform distribution sampling from the hydrological parameter ranges (Table 2) impacts the simulated hydrological extremes.

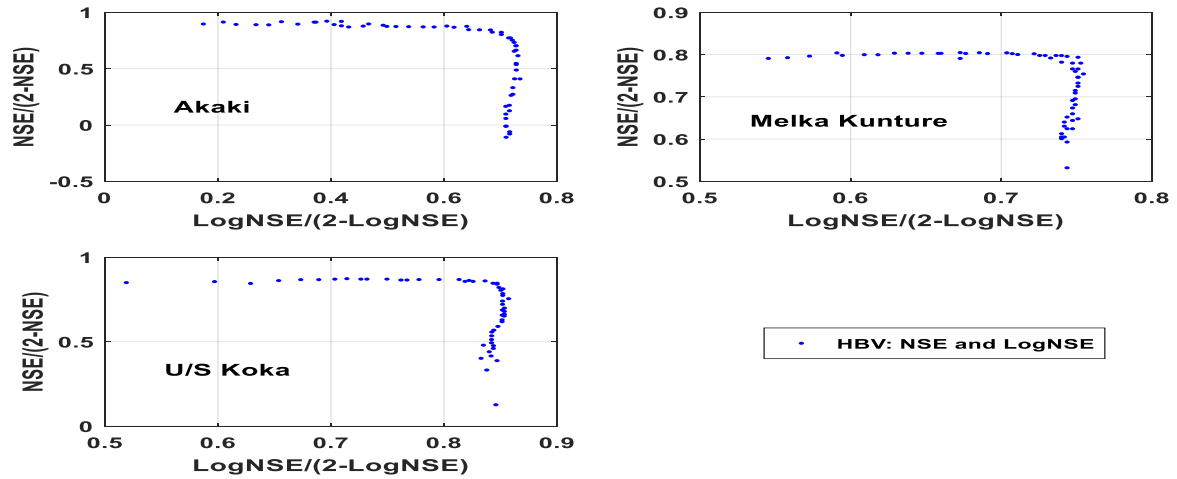


Figure 4. Bounded NSE for peak flow (Y-axis) and LogNSE for low flow evaluation (X-axis) results for three catchments from best/behavioral simulations of HBV hydrological model.

The uncertainty due to the hydrological parameters associated with extreme river flow simulation was estimated using the GLUE approach. We evaluated its role using extreme seasonal indices derived from daily river flow time series and presented it in Figure 6. It is clearly seen that the 95% CI parameters sets were lacking to capture the extreme values characteristics and the very extreme low values. Particularly, U/S Koka catchment has very high events, and these models lacked to simulate these peaks due to the fact that the catchment has a significant backwater and groundwater effect. While, Akaki and MelkaKunture catchments is Ephemeral River and without prolonged dry season, the low and high flow simulation was 100% in the 95% CI. This is due to the model parameter sets and may provide important information in the estimation of uncertainty. This indicates that low flow simulations in short memory catchments are challenging due to their prolonged dry conditions. For the estimation of peak flows, the uncertainty comes from the observed time series characteristics (the number of events). For example, if the catchment has few extremes, the model gives a smaller band, but few extremes fall outside the 95% CI band. A single parameter model is not able to consider all the processes in a watershed. Therefore, no perfect and universally applicable hydrological model and uncertainty estimation are essential to building extreme flow prediction confidence.

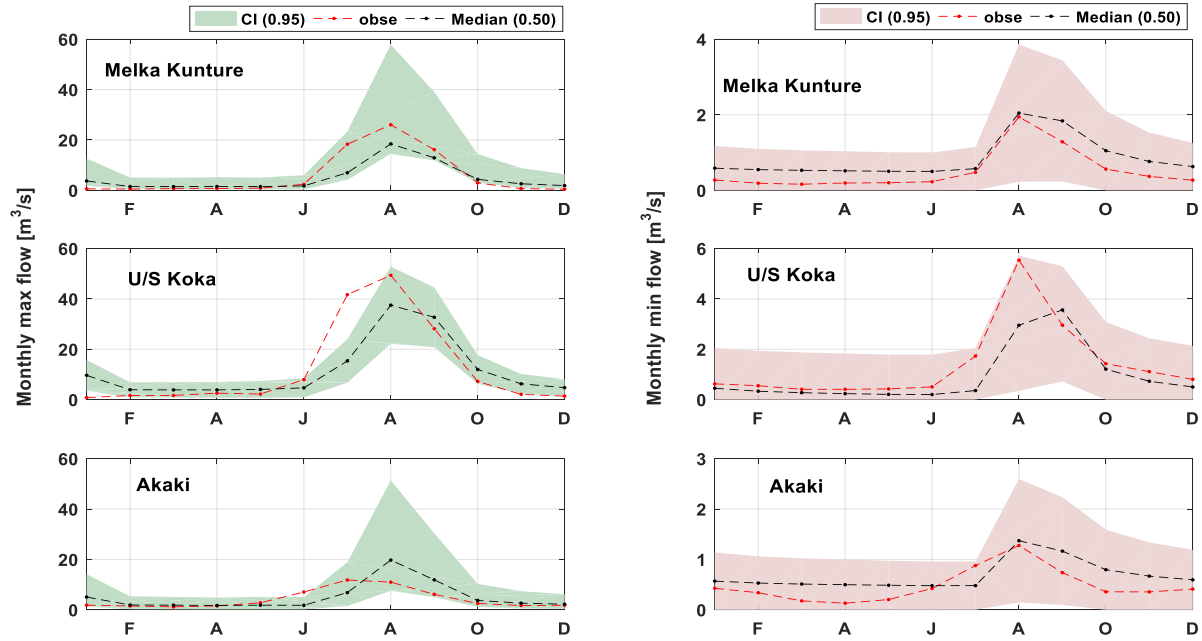


Figure 5. Hydrological parameter uncertainty and its band on simulation of extreme monthly high flow (left column) and monthly min flow (right column) using HBV model. Each color stands for the 95% confidence interval of 100 simulations from 100 best hydrological parameters. The red dot represents the observed extreme maximum/minimum flow of respective stations, and the black dot stands for the median of the simulated flow.

4.3 Evaluation of role and its associated uncertainty

The role and associated uncertainty aggregated from the input data, hydrological parameters, and extreme frequency distribution models become more prominent. They have significant implications in water resource and flood risk management. The total uncertainty increases as the number of uncertainty sources increases in peak flow and low flow frequency estimation (Figure 7). Each source of uncertainty's potential role is estimated by comparing the 95% CI band in the extreme peak and low flow frequencies. Figure 7, displays the peak flow and low flow frequency curves at a given period. Each source of uncertainty is presented by each color shade (the colors are additive): blue represents input data and for range shaded color for hydrological parameters. Their corresponding median values are presented in solid lines of respective uncertainty bands color: blue line, and orange line, respectively. Similarly, in low flow frequency simulations (Figure 7 – left column), the green shaded area represents input data role and light orange shaded area for hydrological parameters.

The additive way of total uncertainty estimation was presented in Figure 7, and does not simultaneously illustrate both the main variables and their interaction uncertainty sources. It

shows only the role of the main source's factors (input data and hydrological parameters). The aggregated uncertainty source accounted for a significant difference in the estimation of peak flow and low flow quantiles. In peak flow quintiles estimation at different return periods, the input data uncertainty band is higher than the hydrological parameter uncertainty. Hydrological parameters have a slightly higher role in the estimation of low flow magnitude and frequency values. This implies that high-quality input data is important to reduce water resource management uncertainty (Figure 7). The hydrological parameters, input data quality and adequacy, and hydrological model parameters play significant role in the reliability and accuracy of environmental flow simulations (Figure 7 - left column). This has a considerable contribution for decision-makers and water resource managers. Based on the median of each source of uncertainty deviation from the aggregated medium value, the extreme peak flow frequency mainly influenced by the uncertainty that comes from the quality of the input data with 70% contribution, and hydrological parameter sets contributed 30% (Figure 7 – right column). Whereas, in the modeling of low flow frequency, the contributors to the total uncertainty are ranked as the quality of input data (55%) and hydrological parameter sets (45%) (Figure 7 – left column).

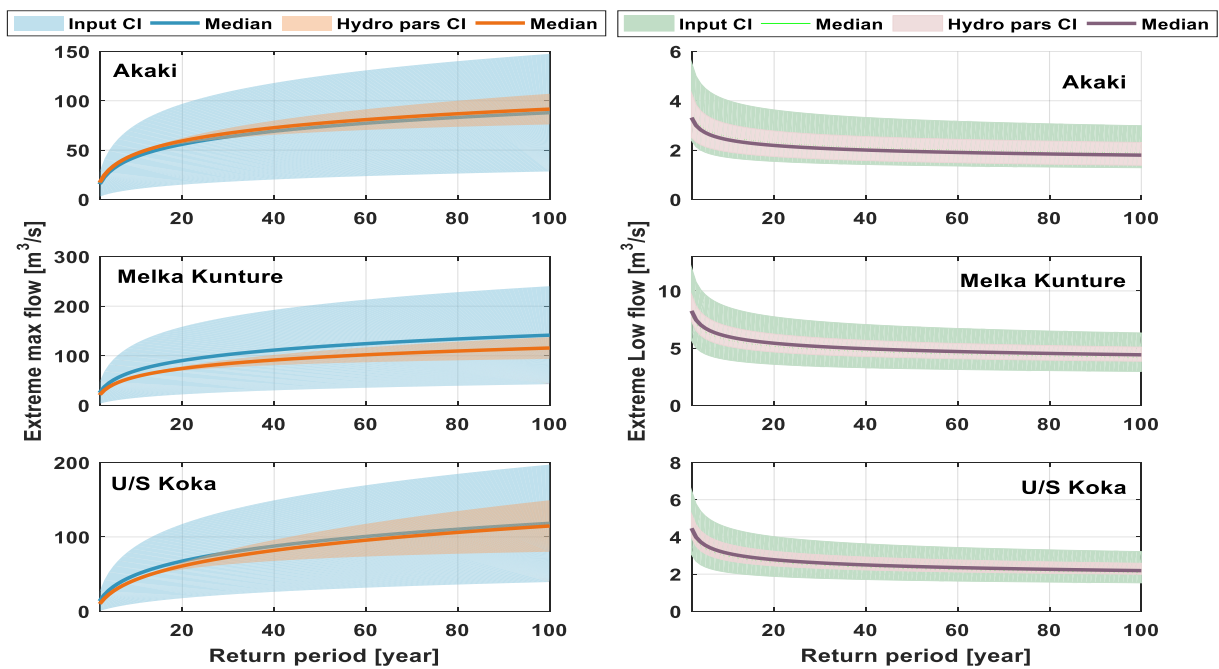


Figure 6. Aggregated uncertainty of peak flow quintile's (left column) and low flow quintile's (right column) for three catchments based on 30 years of simulated data. Each source of uncertainty is presented by each color shade (the colors are additive): blue represents due to input data and for range shaded color for hydrological parameters. Their corresponding median values are presented in solid lines of respective uncertainty bands color: blue line, and orange line, respectively, and in low flow frequency simulations (left column), the green shaded area represents input data role and light orange shaded are for hydrological parameters.

4.4 Uncertainty decomposition using their variances

Variance-based uncertainty decomposition is helpful to understand the interaction of the primary sources of uncertainty. Figure 8 shows the variance decomposition results and provides each variable's percentile contribution and its interaction role in extreme flow simulation. For peak and low flow quintile's at the 10-year return period (QT10) and the peak flow quintile at the 90-year return period (QT90), two main variables and their interactions were identified using ANOVA (Figure 8). These values were derived from two main flow simulations, weighted by LogNSE and NSE likelihood. The variance-based sensitivity analysis results presented in Figure 8 confirm our earlier results on the major influences of the input data spread on the magnitude of high flow quantile (QT90) and supreme influence of hydrological parameters on the magnitude of low flow quantile (QT10). Even though, Figure 7 and Figure 8 show that the main variables have a massive impact on estimating low flow frequency and peak flow frequency at different return periods. Still, at the same time, the interaction of these variables also played a significant role in the total uncertainty band. In particular, the interaction of the input quality band and extreme frequency models band has a considerable influence on peak flow quintile simulations. Similarly, the interaction of hydrological parameters and data inputs has a crucial role in both high and low-flow quantile simulation. The ANOVA analysis result confirms that these two sources of uncertainty's inter-dependency are high and should be considered in water resource modeling and flood risk management.

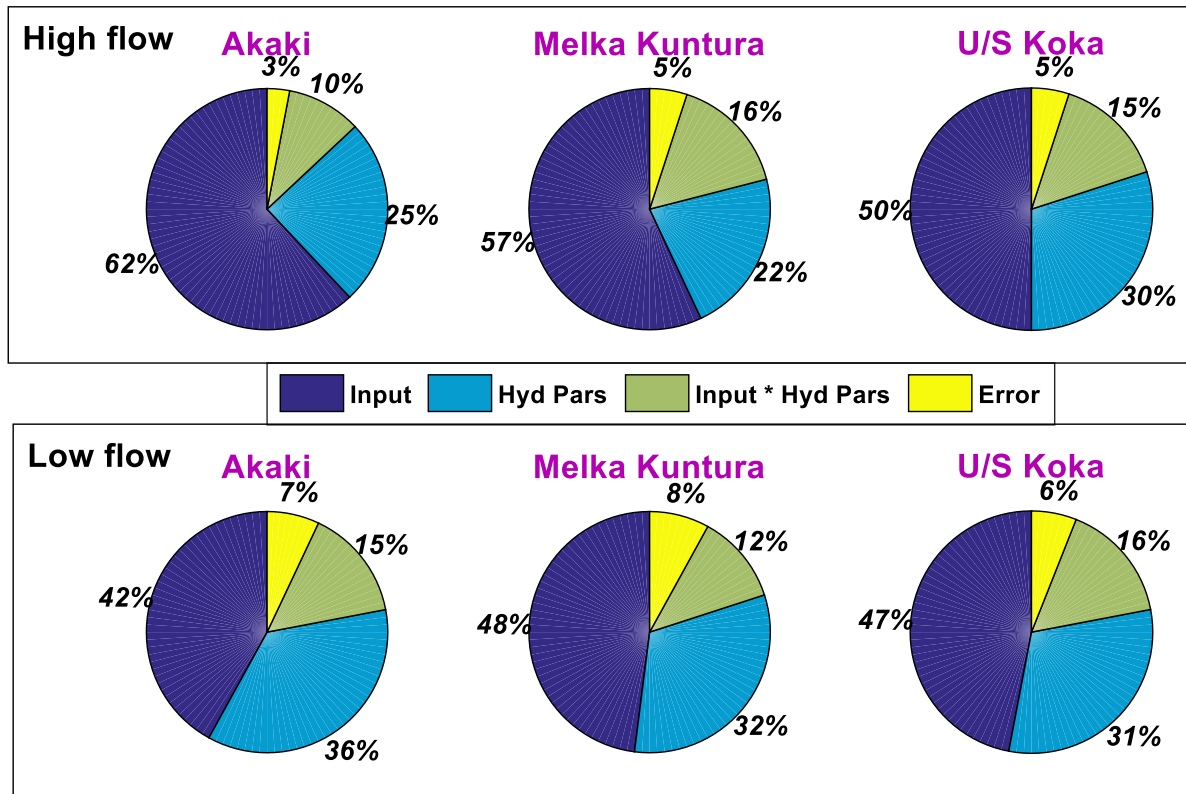


Figure 7. The shares of uncertainty related to Hyd Pars-hydrological parameters and input-input data and their interaction terms (Input*Hyd Pars-hydrological parameters and input data) for the selected three catchments at QT90 (extreme peak flow quantile at 90 years return period – left column) for the selected three catchments at QT10 (extreme low flow quantile at 10-year return period – right column).

The model parameters FC, ALPHA, and BETA CXN, have the highest sensitivity values when the emphasis is made to high flow simulation (i.e., using NSE fitting criteria - Figure 9 (top)); and the HBV model parameters FC, PERC, and KS have the highest sensitivity values when the emphasis is made to low flow simulation (i.e., using logarithm transformation of flow NSE fitting criteria; Figure 9 (bottom)). In general, Figure 9 shows a ranking/sensitivity of the HBV model parameters using the relative maximum vertical difference sensitivity index. The relative importance of the HBV model parameters is shown as ranked from the most sensitive on the left to the least sensitive on the right. The most sensitive parameters in all stations selected as case studies were β and FC. And FC was part of the soil module, and β represented soil moisture variation represented the maximum soil moisture storage, nonlinear routing, respectively. Meanwhile, the least sensitive was WHC in high flow and CFUX in low flow simulations. Moreover, β , the surface runoff component, and soil moisture processes were the most dominant in the mountainous catchments.

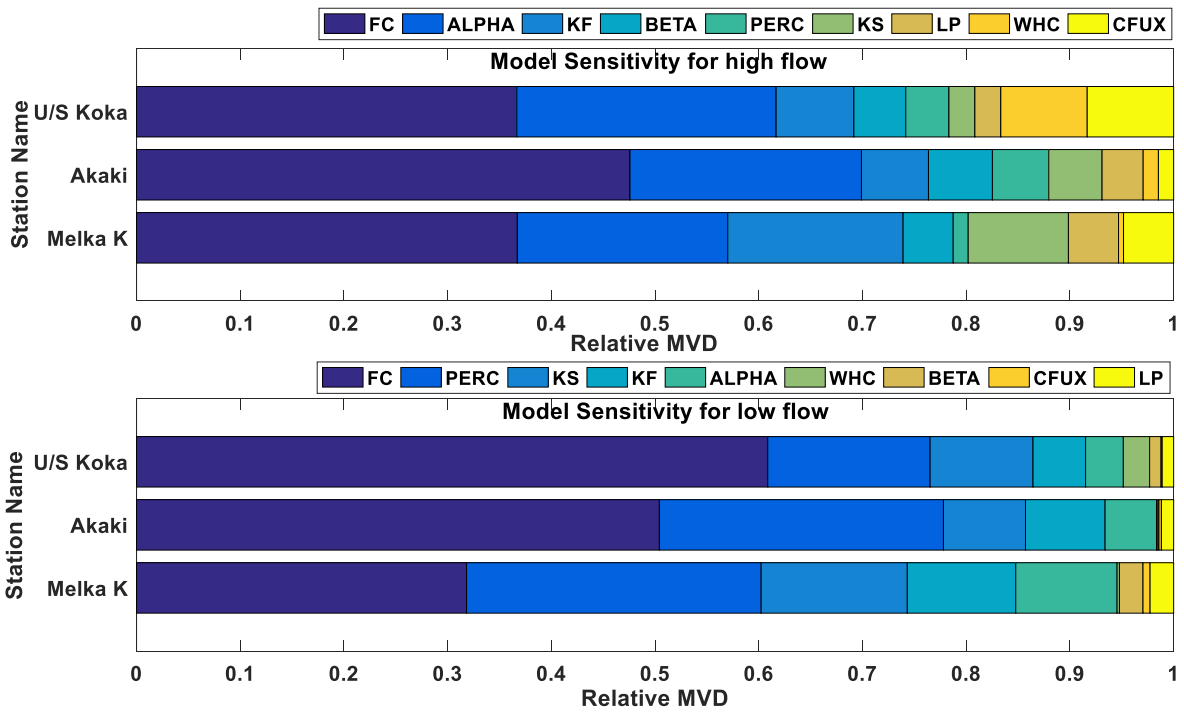


Figure 8. Sensitivity of hydrological model ranks using Relative maximum vertical difference (MVD) values of the HBV model parameters implemented in U/S Koka, Akaki, and Melka K River stations for high flow (upper) and low flow.

5 DISCUSSION

Associated sources of uncertainty and their role in flood and low flow frequency magnitude simulations are quantified. The input uncertainty was established using the generated

realization of precipitation and temperature to address hydrological simulations' reliability. This is a feasible and straightforward approach to improving hydrological simulations. Ajami et al. (2007) also used a similar way of input uncertainty estimation. Still, the model's concept was only applied for precipitation variables under unknown mean and variance, leading to bias in sampling and unrealistic ensembles. The accuracy of generated climate realizations was evaluated against the observed data and the capacity to capture the observed maximum precipitation and temperature time series. The generated realization of climate data was better in Akaki and MelkaKunture than in the U/S Koka catchment. This is related to their lower maximum precipitation events and dry spell length. If the spread of generated precipitation and temperature realization is wide, it will be transferred to the extreme flow, resulting in a wide range in peak or low flow extremes.

The hydrological parameter uncertainty was estimated using GLUE, which is straightforward and frequently used in parameter uncertainty estimation in hydrology (Beven, 2007). In addition to the input data and hydrological model uncertainty, hydrological parameter sets have very significant contributions to the extreme flow frequency. Similarly, Yen et al. (2018); Meresa and Romanowicz, (2017); Bae et al. (2018) also found that the contribution of parameter uncertainty is significant, as presented in this study. However, the role of hydrological parameter sets is not the same for all flow regimes. The peak flow is not significantly influenced by the changing hydrological parameters, while the low flow does. This is because of the model parameters that govern the hydrological water balances slowly and fast flow components. The peak flow component is highly influenced by the snow and soil surface layer-related parameters. In contrast, low flow magnitude is controlled by the snow, surface, and sub-surface soil-related parameters. Overall, the hydrological model showed consistent results and near to the observed peak flow. Similarly, the low flow simulation band value is capsulated the observed low flow values. This is most likely it is due to the influence of physiographic features in the hydrological cycle components (C. Zhang et al., 2016).

In water resource and flood risk management practical exercise, it is mandatory to estimate the peak or low flow frequency using statistical distribution. However, estimates depend on the extreme distribution model (Sun et al., 2017). Hydrological and statistical approaches were combined to estimate the frequency of extreme low and peak flow at three catchments. The result confirms that the frequency distribution uncertainty range (from three distribution types) also significantly contributes to the flood design magnitude. Okoli et al., 2019 et

al.,2019, (2019) found a similar result. These uncertainty sources play an essential role in water resource management and planning, food security, flood risk reduction, poverty reduction, and biodiversity conservation.

The one-line chain from the input to the frequency magnitude of extreme flow at different return periods and total variance-based approach uncertainty decomposition was deployed. The variance-based analysis results showed that input uncertainty has a more considerable contribution to the peak flow frequency magnitude at different return periods. However, using variance-based decomposition (ANOVA), the second more significant contributor is the interaction term of input data and extreme frequency model. Whereas, using a one-line chain, the second considerable contributor is the extreme frequency models. This is due to the lack of consideration of the interaction effect in the one-line chain uncertainty decomposition approach; simultaneously, it is also visible that the ANOVA has an advantage by considering the interaction effect. Similarly, Meresa and Romanowicz, (2017),and Sun et al. (2017) also found the same result. Therefore, these results are associated with the case study areas considered here; however, the framework can be applied elsewhere to evaluate and examine uncertainty for extreme peak and low flow frequency estimation at different return periods.

The proposed comprehensive role evaluation and uncertainty propagation estimation approach are very important for decision-makers and water resource managers. Especially, these results are very mandatory in flood risk modeling and hydrological hazard estimation. Therefore, it would be an important study if researchers focus on how these findings will propagate to risk and drought probability maps. This will be done by integrating these results with the hydrodynamic model to investigate the uncertainty in flood risk and drought probability maps at different return periods.

In this study, the non-stationary characteristics of the hydro climate time series and models have not been considered. Therefore, care is needed to extrapolate uncertainty propagation quantification results to the future or a different time period. If the non-stationary analysis of hydrological parameter and frequency models considered, there are even larger individual uncertainty of both low and peak extremes than those presented.

6 CONCLUSIONS

This study demonstrates the importance of uncertainty propagation quantification in extreme river flow simulation and frequency at different return periods. The associated uncertainty in the extreme frequently modeling depends on the catchment characteristics, adequacy, and quality of forcing data, flow regime, choice of model, and parameterization approach. This newly developed framework is a good and comprehensive lesson that one can learn in extreme risk management and water resource management in most intermediate complexity

catchments. Similarly, it helps to reduce the problem of uncertainty estimation and consideration in practical exercises and natural resource management. The influence of uncertainty on the simulated flow is not uniform across all the selected catchments. Unsurprisingly, the uncertainty in modeling extreme high flow frequency mainly comes from the input data quality. In contrast, in the modeling of low flow frequency, the main contributor to the total uncertainty is model parameter sets uncertainty. This result is also confirmed using ANOVA that adds additional information about the interaction of the main factors. The total uncertainty of QT90 quintile shows that the interaction of input data and extreme frequency models significantly influences the total uncertainty. In the QT10 estimation, the hydrological models and hydrological parameters substantially impact the total uncertainty. In general, input data and its interaction with extreme distribution models are the main factors in modeling extreme peak flow frequency for water resource management and flood risk management. Hydrological parameters and hydrological model structures are the most influential factors in low flow frequency simulation for the purpose of environmental flow modeling and reservoir regulation. This implies that four of the main factors and their interaction may cause significant risk in water resource management and flood and drought risk management. Neglecting these four factors and their interactions may lead to underestimation of risk.

The methodology framework enhanced the procedure for estimating uncertainty and identification by giving a compressive overview and treating possible uncertainty sources in the extreme (flood and drought) frequency magnitude. The results confirm that the framework is sufficient for flood risk managers and modelers, water resource managers, drought disaster risk managers, decision-makers, and ecologists. It gives an outstanding overview and alarms what people should consider and follow.

7 RECOMMENDATIONS

- The role of hydrological parameters and climate input data is significant in flood and low flow estimations and significantly impacts water resources and extremes management.
- Input data dominantly controlled flood magnitude and frequency, whilst the low flow magnitude and frequency were dominantly affected by both input data quality and hydrological parameters.
- It is crucial to consider the main features that cause considerable risk in water resource management and extreme risk management.

- Neglecting the primary factors and their interaction in disaster risk management, water resource planning, and evaluation of environmental impact assessment is not feasible and may lead to considerable risk.
- Improved extreme water management through a complex modeling approach to better prepare for the impact of extreme high and low flow changes are the best long- and short-term plan and strategy to combat and minimize the risk in water-related sectors of the local economy.

8 REFERENCES

- Aldrian, E., Oludhe, C., Garanganga, B. J., Pahalad, J., Rojas-Corradi, M., Boulahya, M. S., Dubus, L., Ebinger, J., & Fischer, M. (2010). Regional climate information for risk management. *Procedia Environmental Sciences*, *1*(1), 369–383. <https://doi.org/10.1016/j.proenv.2010.09.024>
- Andrés-Doménech, I., García-Bartual, R., Montanari, A., & Marco, J. B. (2015). Climate and hydrological variability: The catchment filtering role. *Hydrology and Earth System Sciences*, *19*(1), 379–387. <https://doi.org/10.5194/hess-19-379-2015>
- Antle, J. M. (2008). *Climate Change and Agriculture : Economic Impacts*. *23*(1).
- Austin, J., Zhang, L., Jones, R. N., Durack, P., Dawes, W., & Hairsine, P. (2010). Climate change impact on water and salt balances: An assessment of the impact of climate change on catchment salt and water balances in the Murray-Darling Basin, Australia. *Climatic Change*, *100*(3), 607–631. <https://doi.org/10.1007/s10584-009-9714-z>
- Awulachew, S. B., Wubet, F. D., McCartney, M., & Shiferaw, Y. S. (2011). Hydrological Water Availability, Trends and Allocation in the Blue Nile Basin. In *Nile River Basin*. https://doi.org/10.1007/978-94-007-0689-7_14
- Bae, D. H., Trinh, H. L., & Nguyen, H. M. (2018). Uncertainty estimation of the SURR model parameters and input data for the Imjin River basin using the GLUE method. *Journal of Hydro-Environment Research*, *20*(October 2016), 52–62. <https://doi.org/10.1016/j.jher.2018.05.001>
- Bergström, S. (2006). *Experience from applications of the HBV hydrological model from the perspective of prediction in ungauged basins*. *1995*, 97–107.
- Beven, K., & Beven, K. (2007). *Towards integrated environmental models of everywhere : uncertainty , data and modelling as a learning process*. *11*(1), 460–467.
- BBeven, K., & Binley, A. (2014). *GLUE : 20 years on*. *5918*(November 2013), 5897–5918. <https://doi.org/10.1002/hyp.10082>
- Bewket, W., Radeny, M., & Mungai, C. (2015). Agricultural adaptation and institutional responses to climate change vulnerability in Ethiopia. *CCAFS Working Paper*, *106*, 60-pp. <https://cgspace.cgiar.org/bitstream/handle/10568/56997/Working Paper 106 Final.pdf>
- Breinl, K., Di, G., Girons, M., Hagenlocher, M., Vico, G., & Rutgersson, A. (2017). *Can weather generation capture precipitation patterns across different climates , spatial scales and under data scarcity ? June*, 1–12. <https://doi.org/10.1038/s41598-017-05822-y>
- Burgan, & Aksoy. (2020). Monthly Flow Duration Curve Model for Ungauged River Basins. *Water*, *12*(2), 338. <https://doi.org/10.3390/w12020338>
- Chen, Xi, Yang, T., Wang, X., Xu, C. Y., & Yu, Z. (2013). Uncertainty Intercomparison of Different Hydrological Models in Simulating Extreme Flows. *Water Resources Management*, *27*(5), 1393–1409. <https://doi.org/10.1007/s11269-012-0244-5>

- Clark, M. P., Bierkens, M. F. P., Samaniego, L., Woods, R. A., Uijlenhoet, R., Bennett, K. E., Pauwels, V. R. N., Cai, X., Wood, A. W., & Peters-lidard, C. D. (2017). *The evolution of process-based hydrologic models : historical challenges and the collective quest for physical realism. 1969*, 3427–3440.
- Cunderlik, J. M., Jourdain, V., Quarda, T. B. M. J., Bobée, B., Cunderlik, J. M., Jourdain, V., Quarda, T. B. M. J., & Bobée, B. (2013). *Local Non-Stationary Flood-Duration-Frequency Modelling Local Non-Stationary Flood-Duration-Frequency Modelling. 1784*. <https://doi.org/10.4296/cwrj3201043>
- Desti, H., & Lemma, B. (2017). SWAT based hydrological assessment and characterization of Lake Ziway sub-watersheds, Ethiopia. *Journal of Hydrology: Regional Studies*, 13(March), 122–137. <https://doi.org/10.1016/j.ejrh.2017.08.002>
- Devia, G. K., Ganasri, B. P., & Dwarakish, G. S. (2015). A Review on Hydrological Models. *Aquatic Procedia*, 4(Icwrcoe), 1001–1007. <https://doi.org/10.1016/j.aqpro.2015.02.126>
- Dietrich, J., Trepte, S., Wang, Y., Schumann, A. H., Voß, F., Hesser, F. B., & Denhard, M. (2008). Combination of different types of ensembles for the adaptive simulation of probabilistic flood forecasts: Hindcasts for the Mulde 2002 extreme event. *Nonlinear Processes in Geophysics*, 15(2). <https://doi.org/10.5194/npg-15-275-2008>
- Downer, C. W., & Ogden, F. L. (2003). Prediction of runoff and soil moistures at the watershed scale: Effects of model complexity and parameter assignment. *Water Resources Research*, 39(3). <https://doi.org/10.1029/2002WR001439>
- Emam, A. R., Kappas, M., Fassnacht, S., Hoang, N., & Linh, K. (2018). *Uncertainty analysis of hydrological modeling in a tropical area using different algorithms. 12*(4), 661–671.
- Emerta, B., & Aragie, A. (2013). *C l i m a t e C h a n g e , G r o w t h , and Poverty in Ethiopia. June*.
- EPA. (2017). *An Overview of Rainfall-Runoff Model Types (iEMSs 2018)*. 30.
- Esau, I., Bobylev, L., Donchenko, V., Gnatiuk, N., Lappalainen, H. K., Konstantinov, P., Kulmala, M., Mahura, A., Makkonen, R., Manvelova, A., Miles, V., Pet, T., Fedorov, R., Varentsov, M., Wolf, T., Zilitinkevich, S., & Baklanov, A. (2021). *An enhanced integrated approach to knowledgeable high-resolution environmental quality assessment. 122*(February), 1–13. <https://doi.org/10.1016/j.envsci.2021.03.020>
- ESCAP. (2017). Flood Forecasting and Early Warning in Transboundary River Basins: A Toolkit. *United Nations Economic and Social Commission for Asia and the Pacific*, 83.
- Eumisd, D. (2015). River flow model using artificial neural networks Peer-review under responsibility of the Euro-Mediterranean Institute for Sustainable. *Energy Procedia*, 74(August), 1007–1014. <https://doi.org/10.1016/j.egypro.2015.07.832>
- Fazzini, M., Bisci, C., & Billi, P. (2015). *The Climate of Ethiopia. February 2016*. <https://doi.org/10.1007/978-94-017-8026-1>
- Gao, C., Yao, M. T., Wang, Y. J., Zhai, J. Q., Buda, S., Fischer, T., Zeng, X. F., Yao, M. T., Wang, Y. J., Zhai, J. Q., Buda, S., Fischer, T., & Zeng, X. F. (2016). Hydrological model comparison and assessment : criteria from catchment scales and temporal

- resolution. *Hydrological Sciences Journal*, 61(10), 1941–1951.
<https://doi.org/10.1080/02626667.2015.1057141>
- Gebrehiwot, S. G., Ilstedt, U., Gärdenas, A. I., & Bishop, K. (2011). Hydrological characterization of watersheds in the Blue Nile Basin, Ethiopia. *Hydrology and Earth System Sciences*, 15(1). <https://doi.org/10.5194/hess-15-11-2011>
- Hellin, J., & Fisher, E. (2019). Climate-smart agriculture and non-agricultural livelihood transformation. *Climate*, 7(4), 1–8. <https://doi.org/10.3390/cli7040048>
- Hengl, T. (2007). *A Practical Guide to Geostatistical Mapping of Environmental Variables*.
- IPCC a. (2014). Climate Change 2014 Synthesis Report Summary Chapter for Policymakers. *Ippc*, 31.
- Jain, S. K., Mani, P., Jain, S. K., Prakash, P., Singh, V. P., Tullos, D., Kumar, S., Agarwal, S. P., & Dimri, A. P. (2018). A Brief review of flood forecasting techniques and their applications. *International Journal of River Basin Management*, 16(3), 329–344.
<https://doi.org/10.1080/15715124.2017.1411920>
- Jannis, E., Adrien, M., Annette, A., & Peter, H. (2021). Climate change effects on groundwater recharge and temperatures in Swiss alluvial aquifers. *Journal of Hydrology X*, 11, 100071. <https://doi.org/10.1016/j.hydroa.2020.100071>
- Jenkins, G. M., Reinsel, G. C., Ljung, G. M., Wiley, J., Box, G. E. P., Jenkins, G. M., Reinsel, G. C., Ljung, G. M., & Wiley, J. (2019). *Time Series Analysis : Forecasting and Control , 5th Edition , by George E . P . BOOK REVIEW TIME SERIES ANALYSIS : FORECASTING AND CONTROL ,. March 2016*.
<https://doi.org/10.1111/jtsa.12194>
- Jin, X., Xu, C. Y., Zhang, Q., & Singh, V. P. (2010). Parameter and modeling uncertainty simulated by GLUE and a formal Bayesian method for a conceptual hydrological model. *Journal of Hydrology*, 383(3–4), 147–155. <https://doi.org/10.1016/j.jhydrol.2009.12.028>
- Jury, M. R., & Funk, C. (2013). *Climatic trends over Ethiopia : regional signals and drivers. 1935(August 2012), 1924–1935*. <https://doi.org/10.1002/joc.3560>
- Karakoram, C. (2016). *Predictive Uncertainty Estimation on a Precipitation and Temperature Reanalysis Ensemble for Shigar*. <https://doi.org/10.3390/w8060263>
- Kauffeldt, A., Wetterhall, F., Pappenberger, F., Salamon, P., & Thielen, J. (2016). Environmental Modelling & Software Technical review of large-scale hydrological models for implementation in operational flood forecasting schemes on continental level. *Environmental Modelling and Software*, 75, 68–76.
<https://doi.org/10.1016/j.envsoft.2015.09.009>
- Khazaei, M. R., & Ahmadi, S. (2013). *A new daily weather generator to preserve extremes and low-frequency variability*. 631–645. <https://doi.org/10.1007/s10584-013-0740-5>
- Kiang, J. E., Gazoorian, C., Mcmillan, H., Coxon, G., & Coz, J. Le. (2018). *A Comparison of Methods for Stream flow Uncertainty Estimation*.
<https://doi.org/10.1029/2018WR022708>
- Kidd, C., & Huffman, G. (2011). *Review Global precipitation measurement*. 353, 334–353.
<https://doi.org/10.1002/met.284>

- Koster, R. D., Betts, A. K., Dirmeyer, P. A., Bierkens, M., Bennett, K. E., Déry, S. J., Evans, J. P., Fu, R., Hernandez, F., Leung, L. R., Liang, X., & Masood, M. (2017). *Hydroclimatic variability and predictability : a survey of recent research*. 3777–3798.
- Kourtis, I. M., Kotsifakis, K. G., Feloni, E. G., & Baltas, E. A. (2019). Sustainable water resources management in small greek islands under changing climate. *Water (Switzerland)*, 11(8), 1–19. <https://doi.org/10.3390/w11081694>
- Kusangaya, S., Warburton Toucher, M. L., & van Garderen, E. A. (2018). Evaluation of uncertainty in capturing the spatial variability and magnitudes of extreme hydrological events for the uMngeni catchment, South Africa. *Journal of Hydrology*, 557. <https://doi.org/10.1016/j.jhydrol.2018.01.017>
- Li, L., Xu, C., Xia, J., Engeland, K., & Reggiani, P. (2011). *Uncertainty estimates by Bayesian method with likelihood of AR (1) plus Normal model and AR (1) plus Multi-Normal model in different time-scales hydrological models*. 406, 54–65. <https://doi.org/10.1016/j.jhydrol.2011.05.052>
- Machiwal, D., & Jha, M. K. (2008). Comparative evaluation of statistical tests for time series analysis: Application to hydrological time series. *Hydrological Sciences Journal*, 53(2), 353–366. <https://doi.org/10.1623/hysj.53.2.353>
- Machiwal, D., & Jha, M. K. (2012). Hydrologic time series analysis: Theory and practice. In *Hydrologic Time Series Analysis: Theory and Practice*. <https://doi.org/10.1007/978-94-007-1861-6>
- Maity, R. (2018). Statistical Methods in Hydrology and Hydroclimatology. In *Springer*. <https://doi.org/10.1007/978-981-10-8779-0>
- Malone, T., Davidson, M., Digiacomio, P., Gonçalves, E., Knap, T., Muelbert, J., Parslow, J., Sweijd, N., Yanagai, T., & Yap, H. (2010). Climate change, sustainable development and coastal ocean information needs. *Procedia Environmental Sciences*, 1(1), 324–341. <https://doi.org/10.1016/j.proenv.2010.09.021>
- Martinez, R., Garanganga, B. J., Kamga, A., Luo, Y., Mason, S., Pahalad, J., & Rummukainen, M. (2010). Regional climate information for risk management: Capabilities. *Procedia Environmental Sciences*, 1(1), 354–368. <https://doi.org/10.1016/j.proenv.2010.09.023>
- Marton, D., & Paseka, S. (2017). *Uncertainty Impact on Water Management Analysis of Open Water Reservoir*. February. <https://doi.org/10.3390/environments4010010>
- Masia, S., Sušnik, J., & Trabucco, A. (2018). *Assessment of Irrigated Agriculture Vulnerability under Climate Change in Southern Italy*. 1–19. <https://doi.org/10.3390/w10020209>
- Mason, D. C., Garcia-Pintado, J., Cloke, H. L., & Dance, S. L. (2015). The potential of flood forecasting using a variable-resolution global digital terrain model and flood extents from synthetic aperture radar images. *Frontiers in Earth Science*, 3(August), 1–14. <https://doi.org/10.3389/feart.2015.00043>
- McCuen, R. H. (2016). Modeling hydrologic change: Statistical methods. In *Modeling Hydrologic Change: Statistical Methods*. <https://doi.org/10.1198/tech.2003.s170>
- McGregor, G. (2017). Hydroclimatology, modes of climatic variability and stream flow, lake

- and groundwater level variability: A progress report. *Progress in Physical Geography*, 41(4), 496–512. <https://doi.org/10.1177/0309133317726537>
- Melsen, L. A. (2017). *Putting hydrological modelling practice to the test*. 170.
- Meresa, H.K. (2019). River flow characteristics and changes under the influence of varying climate conditions. *Natural Resource Modeling*. <https://doi.org/10.1111/nrm.12242>
- Meresa, H.K., & Romanowicz, R. J. (2017). The critical role of uncertainty in projections of hydrological extremes. *Hydrology and Earth System Sciences*, 21(8). <https://doi.org/10.5194/hess-21-4245-2017>
- Meresa, Hadush K, & Gatachew, M. T. (2016). Modeling of Hydrological Extremes Under Climate Change Scenarios in The Upper Blue Nile River Basin, Ethiopia. *Journal of Civil & Environmental Engineering*, 06(05). <https://doi.org/10.4172/2165-784x.1000252>
- Meresa, Hadush K, & Gatachew, M. T. (2018). Climate change impact on river flow extremes in the Upper Blue Nile River basin. *Journal of Water and Climate Change*, jwc2018154. <https://doi.org/10.2166/wcc.2018.154>
- Meresa, Hadush K, Romanowicz, R. J., & Napiorkowski, J. J. (2017). Understanding changes and trends in projected hydroclimatic indices in selected Norwegian and Polish catchments. *Acta Geophysica*, 65(4), 829–848. <https://doi.org/10.1007/s11600-017-0062-5>
- Mockler, E M, Chun, K. P., Sapriza-azuri, G., Bruen, M., & Wheeler, H. S. (2016). Advances in Water Resources Assessing the relative importance of parameter and forcing uncertainty and their interactions in conceptual hydrological model simulations. *Advances in Water Resources*, 97, 299–313. <https://doi.org/10.1016/j.advwatres.2016.10.008>
- Newman, A. J., Stone, A. G., Saharia, M., Holman, K. D., Addor, N., & Clark, M. P. (2021). *Identifying Sensitivities in Flood Frequency Analyses using a Stochastic Hydrologic Modeling System*. March, 1–29.
- Okoli, K., Mazzoleni, M., Breinl, K., & Di Baldassarre, G. (2019). A systematic comparison of statistical and hydrological methods for design flood estimation. *Hydrology Research*, 50(6), 1665–1678. <https://doi.org/10.2166/nh.2019.188>
- Pachauri, R. K. (2014). *Climate Change 2014 Synthesis Report*.
- Pechlivanidis, I. G., Arheimer, B., Donnelly, C., Hundecha, Y., Huang, S., Aich, V., Samaniego, L., Eisner, S., & Shi, P. (2017). Analysis of hydrological extremes at different hydro-climatic regimes under present and future conditions. *Climatic Change*, 141(3), 467–481. <https://doi.org/10.1007/s10584-016-1723-0>
- Petersen, L. K. (2019). *Impact of Climate Change on Twenty-First Century Crop Yields in the U . S .* 1–17. <https://doi.org/10.3390/cli7030040>
- Prein, A. F. (2019). *Can We Constrain Uncertainty in Hydrologic Cycle Projections ?* *Geophysical Research Letters*. 2018, 3911–3916. <https://doi.org/10.1029/2018GL081529>
- Ramdane, A. (2014). Human influence on changes in the distribution of land precipitation.

- Journal of Hydrology*, 511, 589–593. <https://doi.org/10.1016/j.jhydrol.2014.02.016>
- Rezaie-Balf, M., Nowbandegani, S. F., Samadi, S. Z., Fallah, H., & Alaghmand, S. (2019). An ensemble decomposition-based artificial intelligence approach for daily streamflow prediction. *Water (Switzerland)*, 11(4). <https://doi.org/10.3390/w11040709>
- Romali, N. S., & Yusop, Z. (2017). *Frequency Analysis of Annual Maximum Flood for Segamat River. 04003*.
- Scott, D., & Lemieux, C. (2010). Weather and climate information for tourism. *Procedia Environmental Sciences*, 1(1), 146–183. <https://doi.org/10.1016/j.proenv.2010.09.011>
- Shawul, A. A., Chakma, S., & Melesse, A. M. (2019). The response of water balance components to land cover change based on hydrologic modeling and partial least squares regression (PLSR) analysis in the Upper Awash Basin. *Journal of Hydrology: Regional Studies*, 26(November). <https://doi.org/10.1016/j.ejrh.2019.100640>
- Song, X., Zhang, J., Zhan, C., Xuan, Y., Ye, M., & Xu, C. (2015). Global sensitivity analysis in hydrological modeling : Review of concepts , methods , theoretical framework , and applications. *JOURNAL OF HYDROLOGY*, 523(225), 739–757. <https://doi.org/10.1016/j.jhydrol.2015.02.013>
- Sood, A., & Smakhtin, V. (2015a). Revue des modèles hydrologiques globaux. *Hydrological Sciences Journal*, 60(4), 549–565. <https://doi.org/10.1080/02626667.2014.950580>
- Sun, H., Jiang, T., Jing, C., Su, B., & Wang, G. (2017). Uncertainty analysis of hydrological return period estimation, taking the upper Yangtze River as an example. *Hydrology and Earth System Sciences Discussions, February*, 1–26. <https://doi.org/10.5194/hess-2016-566>
- Tadese, M. T., Kumar, L., Koech, R., & Zemadim, B. (2019). *Hydro-Climatic Variability : A Characterisation and Trend Study of the Awash River Basin , Ethiopia*.
- Tall, A., Coulibaly, J. Y., & Diop, M. (2018). Do climate services make a difference? A review of evaluation methodologies and practices to assess the value of climate information services for farmers: Implications for Africa. *Climate Services*, 11(June), 1–12. <https://doi.org/10.1016/j.cliser.2018.06.001>
- Taye, M. T., & Willems, P. (2012). Temporal variability of hydroclimatic extremes in the Blue Nile basin. In *Water Resources Research* (Vol. 48, Issue 3). <https://doi.org/10.1029/2011WR011466>
- Taylor, P. (2009). *Hydro climatic disasters in water resources management*. <http://www.unisdr.org/we/inform/publications/10358>
- Tessema, S. M. (2011). *H YDROLOGICAL MODELING AS A TOOL FOR SUSTAINABLE WATER RESOURCES MANAGEMENT : A CASE STUDY OF THE A WASH R IVER B ASIN* (Issue May).
- Ul, M., Omar, H., & Zahra, H. (2019). Selecting the best probability distribution for at - site flood frequency analysis ; a study of Torne River. *SN Applied Sciences*, 1(12), 1–10. <https://doi.org/10.1007/s42452-019-1584-z>
- van den Hurk, B. J. J. M., Bouwer, L. M., Buontempo, C., Döscher, R., Ercin, E., Hananel, C., Hunink, J. E., Kjellström, E., Klein, B., Manez, M., Pappenberger, F., Pouget, L.,

- Ramos, M. H., Ward, P. J., Weerts, A. H., & Wijngaard, J. B. (2016). Improving predictions and management of hydrological extremes through climate services. *Climate Services, 1*, 6–11. <https://doi.org/10.1016/j.cliser.2016.01.001>
- Vesely, F. M., Paleari, L., Movedi, E., Bellocchi, G., & Confalonieri, R. (2019). Quantifying Uncertainty Due to Stochastic Weather Generators in Climate Change Impact Studies. *Scientific Reports*, 1–8. <https://doi.org/10.1038/s41598-019-45745-4>
- Vetter, T., Reinhardt, J., Flörke, M., Griensven, A. Van, Hattermann, F., Seidou, O., Su, B., & Vervoort, R. W. (2017). *Evaluation of sources of uncertainty in projected hydrological changes under climate change in 12 large-scale river basins*. 419–433. <https://doi.org/10.1007/s10584-016-1794-y>
- Vrugt, J. A., ter Braak, C. J. F., Clark, M. P., Hyman, J. M., & Robinson, B. A. (2008). Treatment of input uncertainty in hydrologic modeling: Doing hydrology backward with Markov chain Monte Carlo simulation. *Water Resources Research*, 44(12), 1–15. <https://doi.org/10.1029/2007wr006720>
- Weeink, W. H. A. (2010). *THRESHOLDS FOR FLOOD FORECASTING AND WARNING EVALUATION OF STREAMFLOW AND THRESHOLDS FOR FLOOD*. June, 1–89.
- WMO. (2019). *WMO statement on the status of the global climate in 2013*. WMO-No. 1130. Geneva, Switzerland. (Issue 1085). <https://drive.google.com/file/d/0BwdvoC9AeW-jUeEV1cnZ6QURVaEE/edit?usp=sharing>
- World Meteorological Organization. (2013). *Flood Forecasting and Early Warning. Integrated Flood Management Tools Series*. 19, 59.
- Wu, L., Seo, D., Demargne, J., Brown, J. D., Cong, S., & Schaake, J. (2011). Generation of ensemble precipitation forecast from single-valued quantitative precipitation forecast for hydrologic ensemble prediction. *Journal of Hydrology*, 399(3–4), 281–298. <https://doi.org/10.1016/j.jhydrol.2011.01.013>
- Xu, Y. P., Booij, M. J., & Tong, Y. Bin. (2010). Uncertainty analysis in statistical modeling of extreme hydrological events. *Stochastic Environmental Research and Risk Assessment*, 24(5), 567–578. <https://doi.org/10.1007/s00477-009-0337-8>
- Yalew, A. W., Hirte, G., Lotze-campen, H., & Tscharaktschiew, S. (2018). *Climate Change , Agriculture , and Economic Development in Ethiopia*. <https://doi.org/10.3390/su10103464>
- Yen, H., Wang, R., Feng, Q., Young, C., Chen, S., Tseng, W., Wolfe, J. E., White, M. J., & Arnold, G. (2018). *Input uncertainty on watershed modeling : Evaluation of precipitation and air temperature data by latent variables using SWAT*. 122(June), 16–26. <https://doi.org/10.1016/j.ecoleng.2018.07.014>
- Zhang, C., Yan, H., Takase, K., & Oue, H. (2016). *Comparison of the Soil Physical Properties and Hydrological Processes in Two Different Forest Type Catchments 1*. 43(1), 225–237. <https://doi.org/10.1134/S0097807816120034>

9 ANNEX

			Jan	Feb	Mar	apr	may	jun	jul	aug	sep	oct	nov	dec
Melka K	Estimated	Q5	3.726678	1.491883438	1.472694	1.525823	1.489241117	1.762458	6.980138	18.43382	12.91155	4.344701	2.594236	1.893378
	Observed	Q5	0.580425	0.504121667	0.66057	0.7132	0.857295	2.397347	18.28198	26.04144	16.15077	2.94829	0.66829	0.432548
Akaki	Estimated	Q5	9.64879	3.917596449	3.863821	3.864859	4.057793048	4.675549	15.35217	37.49487	32.69477	11.97136	6.276399	4.753495
	Observed	Q5	0.818803	1.624633333	1.658582	2.570818	2.203945	7.943625	41.6736	49.36401	28.17072	7.224235	2.081499	1.390555
U/S														
Koka	Estimated	Q5	5.053668	1.913283719	1.82163	1.733155	1.822632279	1.786676	6.829004	19.73247	11.88387	3.70791	2.634083	2.21861
	Observed	Q5	1.839353	1.518054767	1.171174	1.535355	2.796737093	7.055378	11.83008	10.97853	6.139418	2.518141	1.701981	1.796255
Melka K	Estimated	Q95	0.585975	0.548457092	0.529723	0.516695	0.504257573	0.500515	0.573674	2.044593	1.837804	1.049798	0.763887	0.628262
	Observed	Q95	0.272807	0.188625	0.161362	0.193963	0.200433333	0.227883	0.477053	1.942617	1.28328	0.5628	0.368568	0.26993
Akaki	Estimated	Q95	0.451241	0.333515692	0.275632	0.237493	0.209140465	0.202069	0.360085	2.953167	3.561466	1.209844	0.728972	0.502694
	Observed	Q95	0.626458	0.55235	0.410748	0.408788	0.425165	0.505315	1.729873	5.535058	2.956332	1.426014	1.112564	0.804558
U/S														
Koka	Estimated	Q95	0.568951	0.530684053	0.510762	0.498583	0.487057169	0.478275	0.48034	1.371634	1.164639	0.795498	0.668662	0.594985
	Observed	Q95	0.426647	0.338630933	0.176757	0.130686	0.203131193	0.422304	0.878287	1.276213	0.738025	0.357309	0.355181	0.410597

	preciation			temperature		
	Melka K	Akaki	U/S Koka	Melka K	Akaki	U/S Koka
jan	0.341033353	0.356027	0.283942	27.2951788	26.65198	26.86725
Feb	0.977676476	1.036678	0.990772	29.8849037	29.2417	29.45697
Mar	1.93445729	1.910578	1.84562	33.0075279	32.36433	32.57959
apr	2.374844691	2.285261	2.119711	34.92184296	34.27864	34.49391
may	2.142004651	2.560683	2.273319	33.11668205	32.47348	32.68875
jun	3.69806163	3.974685	3.360593	31.49121349	30.84801	31.06328
jul	9.727400775	9.181747	8.538978	30.83525269	30.19205	30.40732
aug	9.804772389	9.336348	8.93461	31.38683935	30.74364	30.95891
sep	4.401119556	4.636707	3.777384	31.15773212	30.51453	30.7298
oct	0.491358811	0.411728	0.554282	29.48901211	28.84581	29.06108
nov	0.249311359	0.258754	0.113223	26.67914267	26.03594	26.25121
dec	0.088830518	0.101158	0.05834	25.96998502	25.32678	25.54205